Influence of semi- and intermediate-volatile organic compounds (S/IVOC) parameterizations, volatility distributions and aging schemes on organic aerosol modelling in winter conditions

Paolo Giani[1,2,§], Alessandra Balzarini[2], Guido Pirovano[2], Stefania Gilardoni[3], Marco Paglione[3,*], Cristina Colombi[4], Vorne Luigi Gianelle[4], Claudio A. Belis[5], Vanes Poluzzi[6] and Giovanni Lonati[1]

[1]Dipartimento di Ingegneria Civile e Ambientale, Politecnico Milano, Milano, 20133
[2]Ricerca sul Sistema Energetico (RSE), via Rubattino 54, Milano, 20134
[3]Institute of Atmospheric Sciences and Climate (ISAC), National Research Council (CNR), Bologna, I-40129, Italy
[4]ARPA Lombardia, Settore Monitoraggi Ambientali, Milano, 20129
[5]European Commission, Joint Research Centre, Directorate C Energy, Transport and Climate, Air and Climate Unit, Via Enrico Fermi 2749, Ispra (VA) 21027, Italy
[6]ARPAE Emilia-Romagna, CTR Aree Urbane, Bologna 40122, Italy
[§] Now at Department of Civil and Environmental Engineering and Earth Sciences, University of Notre Dame, Notre Dame, IN, USA
*Now at Institute of Chemical Engineering Sciences, Foundation for Research and Technology Hellas (FORTH/ICE-HT), Patras, Greece

Correspondence. Paolo Giani (paolo3.giani@mail.polimi.it)

Abstract. This study presents a high–resolution (5km) set of new simulations performed with CAMx v6.40 over the Po Valley area (Northern Italy), aimed to enhance organic aerosol (OA) levels prediction and to gain insight into the sensitivity of CAMx to different uncertain features of the input setup. In particular, we mainly investigated the role of (i) volatility distributions of organic emissions, (ii) parametrizations of semi– and intermediate–volatile compounds (S/IVOC) emissions and (iii) different aging schemes, by exploiting the latest experimental information available in the recent scientific literature. Model results were validated against two OA–specific datasets, available for both an urban site (Bologna, February 2013) and a rural one (Ispra, March 2013).

We found out a remarkable performance enhancement of modelled OA levels when applying revisions in S/IVOC emission parametrizations together with the new volatility distributions, at both the validation sites. This performance enhancement is associated with a very significant improvement in secondary organic aerosol (SOA) prediction, mainly due to revised IVOC emissions. At Bologna urban site, mean fractional bias (MFB) of OA ranged from -80.1% in the worst run to -10.1% in the best one and index of agreement (IOA) from 0.52 to 0.75. Notable improvements but overall poorer metrics were found for Ispra site, where MFB ranges from -84.2% to -35% and IOA from 0.45 to 0.50. These findings indicate that organic matter in the semi– and intermediate–volatile range are most likely underestimated in official emission inventories for each main source category (i.e. biomass burning, diesel and gasoline vehicles exhaust).

Finally, model results did not show a very pronounced sensitivity to aging processes, due to the low photochemical activity typically observed during winter–time. However, we give evidence that enabling aging processes for biomass burning related SOA, which is by default disabled in CAMx v6.40, can help in closing the gap between modelled and observed SOA concentrations.

Highlights

- Latest experimental studies about emissions of organic matter implemented in CAMx
- Remarkable improvement on modelled organic aerosol levels
- S/IVOC emission revisions appear to be the key factor for such improvement
- Enabling aging processes for biomass burning SOA enhances the performance of the model
- VBS provides a better reconstruction of POA and SOA relative contribution to the total

Keywords. Organic aerosol modelling, CAMx, S/IVOC, VBS, Po Valley

1 Introduction

Atmospheric pollution from particulate matter (PM) represents one of the major environmental and social concern for human health and it poses several challenges in terms of management and mitigation of harmful impacts. According to the latest European Environment Agency report (EEA, 2017), approximately 53% of the EU-28 population was exposed to PM concentrations exceeding the WHO Air Quality Guidance value for PM_{10} (WHO, 2006) in 2015. Premature deaths resulting from such exposure are estimated to be around 400 000 in the EU-28 countries. Nevertheless, the trend of mean PM concentration in Europe is rather flat during the most recent years (Guerreiro, et al., 2014; Barmpadimos, et al., 2012). Development of cost– effective mitigation policies depends heavily upon reliable air quality models results (Harrison, et al., 2008) which can give insights about the impact of a given control strategy on PM concentrations.

A relevant fraction of submicron particulate matter is given by organic aerosol (OA), which accounts for 20–90% of total $PM_{2.5}$ (Zhang, et al., 2007). However, the large complexity of OA chemical composition, with thousands of organic chemical species found in the ambient aerosol (Goldstein & Galbally, 2007), as well as the complex atmospheric processing of organic compounds strongly limited scientific progress in the OA modelling area (Hallquist, et al., 2009; Fuzzi, et al., 2015). Within the atmospheric modelling community, there is mounting evidence that – despite an overall good agreement in gaseous pollutants – OA mass is in most applications underestimated mainly because of the not well reproduced secondary (SOA) fraction (Meroni, et al., 2017; Ciarelli, et al., 2016; Woody, et al., 2016; Zhang, et al., 2013; Bergström, et al., 2012; Hodzic, et al., 2010).

The traditional scheme for OA modelling in Chemical Transport Models (CTMs) is based on the so called "Two-product approach" by Odum et al. (1996). This approach considers primary organic aerosol (POA) that is directly emitted from various combustion sources (e.g. vehicles exhaust, biomass burning) as a non–volatile species that does not chemically evolve. SOA is formed from the early generation oxidation of gaseous organic volatile (VOC) precursors, which produces two nonreactive semi-volatile products that are partitioned between gas and aerosol phases depending on temperature and OA mass concentration. However, recent experimental studies highlighted that this approach presents two main limitations. First, Robinson et al. (2007) suggested that POA species should be treated as semi-volatile compounds that can evaporate from the particulate phase, react in the gas-phase and repartition as SOA, as pointed out also in other works (Jimenez, et al., 2009; Grieshop, et al., 2009). In the conceptual model of Robinson et al. (2007), POA emission is associated with semi–volatile (SVOC) and intermediate–volatile (IVOC) compounds emissions. SVOC compounds are characterized by a relatively low volatility (effective saturation concentration C* between 10^{-1} and 10^{3} μg m^{-3}) and are in the substantial partitioning with the particulate phase whereas IVOC compounds (C* between 10^{3} and 10^{6} μg m^{-3}) are highly volatile and they partition preferentially to the gas-phase in atmospheric conditions..

The second main issue of Odum et al. (1996) approach is related to the further oxidation of SOA in the atmosphere (i.e., the so-called aging process), which is traditionally neglected as the products of VOC oxidation were considered non–reactive. These two limitations led to the development of a new framework for the description of all OA components and their reactions. This new framework – in literature referred to as VBS (Volatility Basis Set) – rethinks the distinction between the traditional primary and secondary OA by grouping organic species into surrogates according to their volatility and degree of oxidation, thus providing a more realistic picture of the behavior of atmospheric organic aerosol. Details about theoretical aspects of VBS framework are provided in Donahue et al. (2006); Donahue et al. (2011); Donahue et al. (2012b).

Several applications of the VBS scheme to CTMs in different case studies can be found in the recent scientific literature (Fountoukis, et al., 2011; Tsimpidi, et al., 2011; Bergström, et al., 2012; Zhang, et al., 2013; Fountoukis, et al., 2014; Koo, et al., 2014; Ciarelli, et al., 2016; Woody, et al., 2016; Fountoukis, et al., 2016; Meroni, et al., 2017). The general conclusion stemming from these works is that the VBS scheme enhances the prediction of both OA levels and degree of oxidation, although the high number of parameters to be constrained in the VBS scheme causes a large uncertainty in the models results. For instance, all the studies cited above scaled the IVOC emissions, which are traditionally neglected in official emission inventories (Ots,

et al., 2016; Hodzic, et al., 2010), on POA emissions using a factor between 1.5× and 3×, as suggested by Robinson et al. (2007). However, this assumption historically derives from chassis dynamometer tailpipe measurements performed two decades ago on two diesel vehicles (Schauer, et al., 1999) and – whilst it might hold true for vehicles exhaust emissions (Kim et al., 2016) – it is likely to be incorrect for other emissions sources (e.g. biomass burning, Ciarelli et al., 2017b). Very recent experimental works presented more detailed and source-specific parametrizations for IVOC emissions, which might be implemented in CTMs to provide more accurate results. As an example, Jathar et al. (2014) performed smog chamber experiments to investigate SOA formation from gasoline vehicles, diesel vehicles and biomass burning, and they reported that unspeciated organics – which are not appropriately included in current emission inventories and, in turn, chemical transport models – account for 10–20% of total non-methane organic gases (NMOG). Zhao et al. (2015) and Zhao et al. (2016) characterized emissions of IVOC from on-road and off-road diesel and gasoline vehicles during dynamometer testing, respectively, reporting both new volatility distributions of the organics emissions and new parametrizations for IVOC emissions calculation. Ciarelli et al. (2017b) performed novel smog chamber experiments for wood combustion emissions, and their result suggest an average ratio of non–traditional VOCs (i.e. IVOC) to POA emissions of 4.75, much higher compared to the widely adopted 1.5, which however was based on diesel vehicles measurements.

Recent European modelling studies attempted to integrate these new parametrizations into CTMs. Ciarelli et al. (2017a) constrained a modified VBS scheme to treat biomass burning OA and evaluated the implementation of this scheme in CAMx. Ots et al. (2016) and Sartelet et al. (2018) investigated different parametrizations for traffic-related S/IVOC emissions for the UK and the greater Paris area, respectively. Chrit et al. (2018) addressed both biomass burning and traffic-related S/IVOC emission parametrizations, volatility distributions and aging by performing a set of sensitivity simulations over western Mediterranean region during winter time. The overall outcome of these works is that updating S/IVOC emission parametrizations and volatility distributions helps in closing the gap between observed and predicted OA concentrations.

Here, we present a new set of sensitivity simulations with CAMx that, differently from previous studies, aims to evaluate model performances in conditions where high OA levels are measured. Following the most recent European studies, we investigate the impact of volatility distributions of organics emissions, S/IVOC emission parametrizations, SOA yields from gaseous precursors and different aging schemes, by implementing the latest experimental information available in the scientific literature. The study area is the Po Valley (Northern Italy) during wintertime (February-March 2013), which is a well-known hotspot where PM levels remain problematic despite the air quality remediation plans intended to get in compliance with current EU air quality standards, mainly because of adverse meteorological conditions (Caserini, et al., 2017; Perrino, et al., 2014; Pernigotti, et al., 2012; Ferrero, et al., 2011). We evaluate our model results against two OA–specific datasets, available for both an urban site (Bologna, February 2013) and a rural one (Ispra, March 2013). These two datasets are derived from Positive Matrix Factorization (PMF) analysis of Aerosol Mass Spectrometer (AMS) and Aerosol Chemical Speciation Monitor (ACSM) measurements (DeCarlo, et al., 2006; Ng, et al., 2011), which allow a thorough comparison of each fraction of organic aerosol (i.e. primary and secondary). We also point out how the development of different meteorological condition can influence the overall model performance as well as, more specifically, the reconstruction of the organic fraction.

2 Methods

2.1 The modelling setup

CAMx v6.40 (ENVIRON, 2016) was used to calculate the concentrations of both gaseous and particulate pollutants over the Po Valley domain, for a two-month long period covering February and March 2013. OA concentrations can be computed by CAMx v6.40 with three different schemes: (i) a traditional two–product model, which is called SOAP in CAMx (Strader, et al., 1999), (ii) the same two–product model with revised

yields for SOA production (SOAP2), based on new aerosol yield data that accounts for vapor wall losses in chamber experiments (Zhang, et al., 2014; Hodzic, et al., 2016) and (iii) a 1.5D–VBS scheme, which is widely described in Koo et al. (2014). SOAP and SOAP2 algorithms treat POA as non–reactive and non–volatile, and compute SOA concentrations starting from VOC and IVOC oxidation. VBS scheme instead employs four basis sets, two for primary aerosols from anthropogenic sources (PAP*x*) and biomass burning (PFP*x*) and two for secondary aerosols, again with the distinction between anthropogenic (PAS*x*) and biomass burning (PBS*x*) origin. It should be noted that the biomass burning category includes also anthropogenic emissions deriving from residential wood heating, which accounts for an important share of total PM emissions during winter time in the Po Valley area (Guariso & Sangiorgio, 2018; Pietrogrande, et al., 2015). Each set has five different volatility bins (*x* ranges from 0 to 4, e.g.: PAP0, PAP1, up to PAP4) equally spaced on a logarithmic scale of effective saturation concentration, covering the whole semi–volatile range, i.e. C* = {0, 1, 10, 100, 1000} µg m^{-3}. An effective saturation concentration equal to zero means a non–volatile bin. Under this framework, total POA concentration is the sum of PAP*x* and PFP*x* and total SOA concentration is the sum of PAS*x* (ASOA, i.e. anthropogenic SOA) and PBS*x* (BSOA, i.e. biomass burning and biogenic SOA). Total OA is the sum of POA and SOA.

The overall configuration of the modelling chain follows the one presented in Meroni et al. (2017). CAMx v6.40 was applied over two nested domains, the outer covering the whole Italian peninsula with a spatial resolution of 15km and the inner one covering the Po Valley area and small parts of other countries at 5km resolution (Figure 1). CAMx uses 14 terrain–following vertical layers, with thickness varying according to the orography and the distance from the ground. Meteorological input was derived by the output of Weather

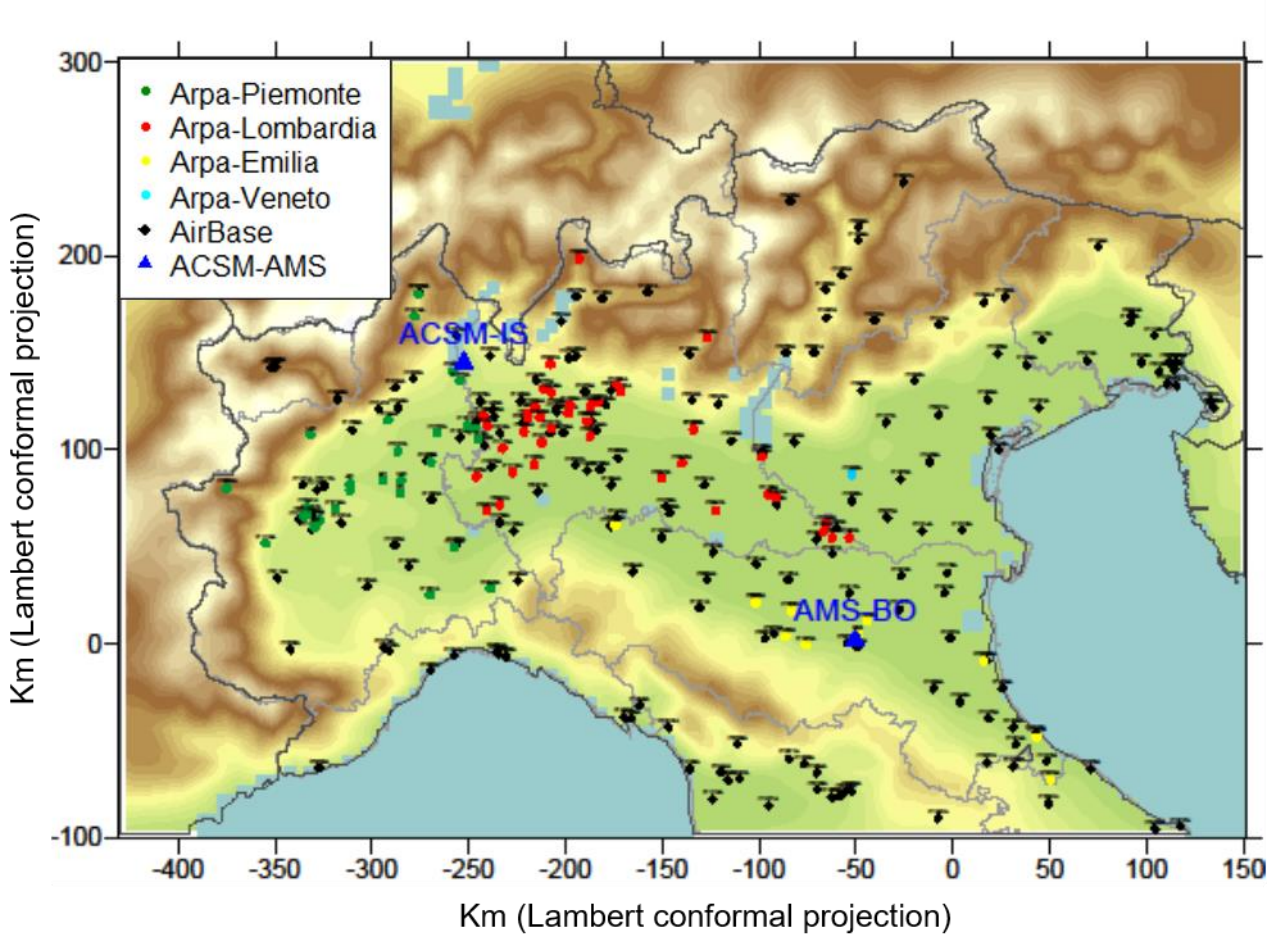

Figure 1 - Air quality measurements sites from both ARPA (circles) and AirBase (diamonds) datasets, in the whole Po Valley domain. Airbase sites are used when both ARPA and AirBase data are available. Different colors stand for different ARPA agencies (i.e. green for ARPA Piemonte, red for ARPA Lombardia, yellow for ARPA Emilia Romagna, cyan for ARPA Veneto). The location of AMS and ACSM sites is reported with blue triangles.

Research and Forecasting model (WRF) (Skamarock, et al., 2008), applied over three nested domains, the largest of which covering Europe and Northern Africa at 45km resolution and the two innermost covering Italy and the Po Valley area at 15km and 5km resolution, respectively. Hourly anthropogenic emission fields were computed by the Sparse Matrix Operator for Kernel Emission model (SMOKE v3.5), which processes inventory data from three different levels (regional, Italian and European data) as in Meroni et al. (2017). Total hourly emission fields were obtained by adding SMOKE fields to biogenic and sea salt emissions, estimated using the Model of Emissions of Gases and Aerosols from Nature (MEGAN v2.03) (Guenther, et al., 2006) and SEASALT model (Gong, 2003), respectively. Additional details about WRF configuration and emission data preparation can be found in Meroni et al. (2017).

2.2 The base case

We first set up a "base case" simulation to be used as a reference to assess the sensitivity of the model to different input features. The configuration of the base case is almost the same as the one described in Meroni et al. (2017), except for a few changes that we implemented in our new base case: (i) the new code version of CAMx (from v6.20 to v6.40), (ii) new gas–phase mechanism (from CB05 to the more recent CB6r4, ENVIRON, 2016), (iii) update of SMOKE speciation profiles for VOCs to be compatible with the new gas–phase mechanism and (iv) revision of elemental carbon (EC) and organic matter (OM) emission factors with more recent literature data (Caserini, et al., 2013; EMEP, 2016; Yarwood, et al., 2010). We updated the gas–phase mechanism because CB6r4 explicitly adds the gas–phase treatment of some SOA precursors (benzene, acetylene) and a new aromatics chemistry which is relevant to SOA modelling. Finally, Table 1

Table 1 - Comparison of OM and EC mass speciation factors for PM2.5

	Meroni et al. (2017)		Caserini et al. (2013)	
	EC	OM	EC	OM
Wood burning	15.4%	51.0%	11.1%	53.7%
Heavy duty diesel	69.4%	17.5%	49.4%	26.0%
Light duty diesel	69.0%	17.5%	67.8%	19.0%
Diesel passenger	71.1%	16.5%	75.0%	16.2%
Gasoline	19.0%	54.9%	36.5%	53.4%
Tire&Brake wear	6.0%	24.4%	3.7%	21.1%

summarizes the new OM and EC profiles compared to the previous ones, according to the Po Valley–specific work of Caserini et al. (2013).

We performed both a SOAP2 and a VBS simulation with these settings, in order to get a comparison between the two algorithms and to evaluate the effect of the revised yields of SOAP2 algorithm. Labels for the new base case runs are *01_soap2_newbase* and *02_vbs_newbase* for SOAP2 and VBS algorithms, respectively.

2.3 New IVOC parametrizations

The base case simulations compute IVOC emissions with the traditional 1.5×POA parametrization, regardless of the source of the emission. However, as in the last few years many modelling works claimed that accurate IVOC emission estimates are crucial for SOA prediction (Shrivastava, et al., 2011; Bergström, et al., 2012; Meroni, et al., 2017), some experimental works have recently presented more detailed and source-specific parametrizations, which are summarized in Table 2.

Table 2 - Different IVOC source-specific emission parametrizations from recent literature data. GV stands for Gasoline Vehicles, DV for Diesel Vehicles and BB for Biomass Burning.

Reference	Type	Gasoline	Diesel	Biomass
Robinson et al., (2007)	Rev[a]	$1.5 \times POA_{GV}$	$1.5 \times POA_{DV}$	$1.5 \times POA_{BB}$
Jathar et al. (2014)	Rev[a]	$0.25 \times NMOG_{GV}$[c]	$0.20 \times NMOG_{DV}$[c]	$0.20 \times NMOG_{BB}$[c]
Zhao et al. (2015)	Exp[b]	—	$0.6 \times NMHC_{DV}$[c] ($12 \times POA_{DV}$)	—
Zhao et al. (2016)	Exp[b]	$0.04 \times NMHC_{GV}$[c]	—	—
Ots et al. (2016)	Rev[a]	—	2.3xSNAP7[d]	—
Ciarelli et al. (2017b)	Exp[b]	—	—	$4.75 \times POA_{BB}$
Hatch et al. (2017)	Exp[b]	—	—	$0.09 \times NMOG_{BB}$[c]

[a] Review, i.e. the authors propose a new parametrization based on previous works
[b] Experimental study, i.e. the authors propose a parametrization based on new measurements
[c] NMOG = Non-Methane Organic Gases; NMHC = Non-Methane HydroCarbons
[d] SNAP7 refers to the VOC emission from road-transport

Using such parametrizations in our case study leads to very different results in terms of total IVOC emissions. In the base case run, total IVOC emission was approximately 10.6 kton, during February 2013 and considering the whole Po Valley domain. Jathar et al. (2014) parametrization would add a slightly lower amount of IVOC (7.6 kton), but with a different allocation between the different sources, being IVOC scaled on VOC rather than POA. Ots et al. (2016) simulations included additional diesel-related intermediate-volatility organic compound emissions derived directly from ambient measurements at an urban background site in London. Their parametrization would lead, in our case study, to the addition of 22.1 kton of diesel-related emissions, which is 2.09 times the amount in the base case.

However, for our new run we decided to use the most up-to-date actual experimental studies, i.e. direct and source-specific emission measurements. For biomass burning emissions (BB), we used the parametrization of Ciarelli et al. (2017b), which is the most recent European study focused on BB. Gasoline (GV) and diesel (DV) vehicles emission parametrizations were instead borrowed from two American studies (Zhao, et al., 2015; Zhao, et al., 2016) as there are no detailed experimental European works related to IVOC emissions from GV and DV. Emissions of IVOC from other sources were calculated as 1.5×POA, as there are no other information available. In calculating IVOC emissions from GV and DV, we took into account that current emissions inventories only report estimates for VOCs, i.e. $C^* > 10^7$ μg m^{-3} (Ots, et al., 2016), and for the particle fraction of the emissions of species with lower volatilities. As an example, let us consider emissions from gasoline vehicles. Since IVOC are not included in the official emission inventory of VOC, the following relationships hold:

$$\mathrm{IVOC} = 0.04 \times \mathrm{NMHC} \quad \text{(Zhao, et al., 2016)} \tag{1}$$

$$\mathrm{NMHC} = (\mathrm{VOC} + \mathrm{IVOC}) \times 0.954 \tag{2}$$

where the factor 0.954 takes into account the difference between non-methane hydrocarbons and non-methane organic gases, i.e. NMOG = VOC + IVOC and NMHC = 0.954 × NMOG (Gabele, 1997). From (1) and (2), we can easily find that:

$$\mathrm{IVOC} = \frac{0.04 \times 0.954}{1 - 0.04 \times 0.954} VOC \tag{3}$$

We proceeded in the same way for IVOC emissions from diesel vehicles, where the coefficient NMHC/NMOG is equal to 0.934 (EPA, 2005) and the scaling factor on NMHC is 0.6 (Zhao, et al., 2015). IVOC emissions calculation from biomass burning was instead straightforward, as Ciarelli et al. (2017b) parametrization scales

IVOC emissions on POA ones. The resulting total IVOC emission budget using these three parametrizations is 33.8 kton, which is 3.19 times the emission in the base case. The apportionment of these emissions to the different source categories is reported in Table 3. Again, we performed both a SOAP2 and a VBS run with revised IVOC parametrization, keeping the rest of the configuration as the one described in the previous section (i.e., the new base case), to evaluate the effect of adding this IVOC emissions on both algorithms. Labels for these two runs are *03_soap2_newivoc* and *04_vbs_newivoc*.

Table 3 - Source–related and total IVOC emissions according to the revised parametrizations and Meroni et al. (2017) work. All emissions values refer to the Po Valley domain during February 2013 and are reported in tons.

Source	Base case	Revised	Revised/Traditional
Gasoline vehicles	119.9	276.1	2.30
Diesel vehicles	556.3	3137.2	5.64
Biomass burning	9461.3	29 960.8	3.17
Others	462.5	462.5	1.00
Total	10600.1	33836.6	3.19

2.4 New volatility distributions and OM_{SV} estimates

In all the above–mentioned runs, we implicitly assumed that POA = OM_{SV}, where OM_{SV} is the organic matter in the semi-volatile range. We basically allocated POA emissions from the official inventory into the five volatility basis sets (C* = {0, 1, 10, 100, 1000} µg m^{-3}) via the default volatility distributions of CAMx, which are borrowed from May et al. (2013a); May et al. (2013b); May et al. (2013c); Woody et al. (2015). However, as already mentioned before, several studies showed that this assumption might not hold true (Shrivastava, et al., 2011; Tsimpidi, et al., 2010; Ciarelli, et al., 2016) and new volatility distributions are now available in the recent literature. Many modelling works therefore performed some sensitivity runs in which OM_{SV} was increased by a factor 1.5×, 2× , 3× (Shrivastava, et al., 2011; Tsimpidi, et al., 2010; Ciarelli, et al., 2016). Nevertheless, instead of using fixed factors (i.e. with no physical meaning) as in previous studies, we decided to infer OM_{SV} with the most recent information available and then to compare it with the official values from the emission inventory. For gasoline and diesel vehicles emissions, we calculated OM_{SV} starting from the volatility distribution provided in Zhao et al. (2015); Zhao et al. (2016), respectively, being known the ratio (R) between IVOC and OM_{SV} (Figure 2). OM_{SV} can be thus calculated as IVOC/R.

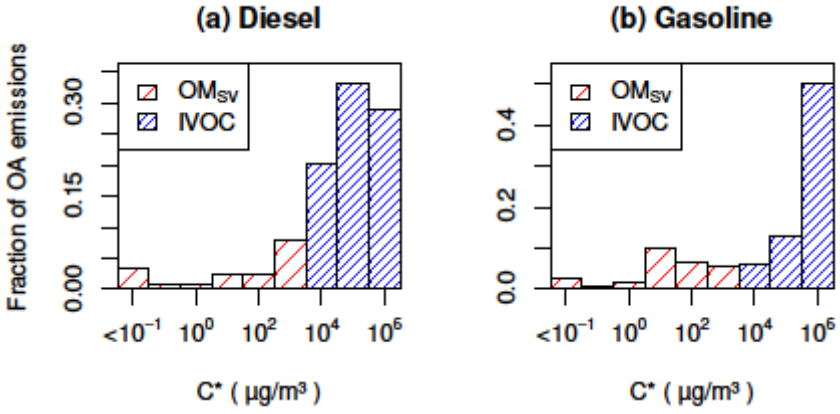

Figure 2 - Diesel (a) and gasoline (b) complete volatility distributions (Zhao, et al., 2015; Zhao, et al., 2016). The ratio R is the sum of the IVOC bars divided by the sum of the OM_{SV} bars (R = 4.62 for gasoline emissions and R = 2.54 for diesel emissions).

For biomass burning, since we did not have an updated volatility distribution covering the whole semi– and intermediate–volatile range, we used a factor from the revised inventory of Denier van der Gon et al. (2015), which takes into account also condensable organics. The ratio between OM in the inventory of Denier van der Gon et al. (2015) and OM in our emission inventory, considering BB emissions for the whole Italy, is 1.34 and

therefore we scaled up BB emissions using this correction factor. Table 4 summarizes the results of these revisions in terms of total emission for February 2013 and the whole Po Valley domain. As clear from Table 4, all the calculated OM_{SV} are actually higher than traditional POA emission, confirming that current emission inventories are probably missing SVOC emissions.

Table 4 - Comparison between official inventory data of OM_{SV} (i.e. POA) and the revised OM_{SV} according to our methodology. All emissions values refer to the Po Valley domain during February 2013 and are reported in tons.

Source	Official OM_{SV}	Revised OM_{SV}	Revised/Official
Gasoline vehicles	80.0	108.8	1.36
Diesel vehicles	370.9	679.3	1.83
Biomass burning	6307.5	8452.1	1.34

Finally, in addition to the revised emission of OM_{SV}, we also applied the new volatility distributions from Zhao et al. (2015); Zhao et al. (2016) for gasoline and diesel emissions as well as the IVOC parametrizations as in *04_vbs_newivoc*. The comparison between default and updated volatility distributions is shown in Figure 3. With respect to the default volatility distributions, DV emissions are mostly associated with the lowest and highest C* bins in the semi-volatile range whereas GV emissions present a general shift towards higher volatilities.

This new run will be hereinafter referred to as *05_vbs_newomsv*. As we are assessing the influence of VBS–specific parameters (i.e. volatility distributions), no equivalent SOAP2 run has been performed.

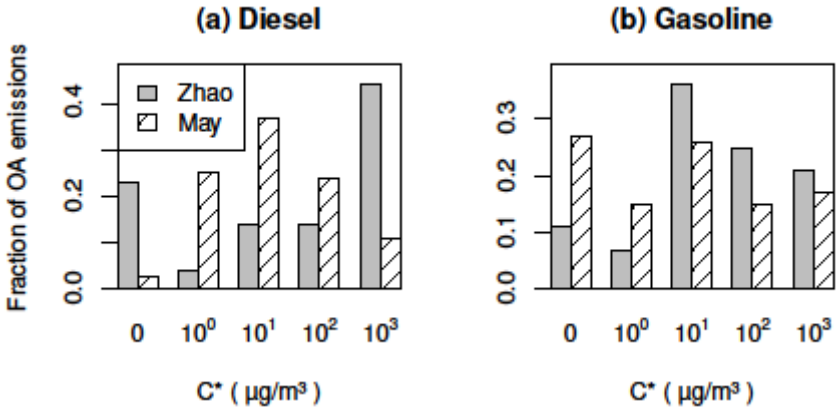

Figure 3 - Comparison of volatility distributions in the semi–volatile range between Zhao et al. (2015); Zhao et al. (2016) and CAMx default (May, et al., 2013a; May, et al., 2013b; May, et al., 2013c) for (a) diesel emissions and (b) gasoline emissions.

2.5 Model sensitivity to aging schemes

In Meroni et al. (2017) and all the above-mentioned runs, multigenerational aging scheme has been borrowed from Koo et al. (2014) which is the default in CAMx. Chemical aging process is approximated by using a partial conversion from POA to SOA, i.e. oxidation products of POA aging are a mixture of POA and SOA in the next lower volatility bin. The mixture ratios (i.e. how much POA/SOA is produced from each oxidation reaction) are calculated via carbon and oxygen balances and are provided in Koo et al. (2014). A rate constant of 4×10^{11} cm^3 $molecule^{-1}$ s^{-1} is used for gas-phase oxidation of POA with OH radical (Robinson, et al., 2007). The OH reaction rate for anthropogenic SOA is assumed to be 2×10^{11} cm^3 $molecule^{-1}$ s^{-1}. Aging of SOA deriving from biomass burning and biogenic precursors (BSOA) is instead disabled in default CAMx configuration based on previous modelling studies which found that aging of BSOA led to overestimation of OA in rural areas (Lane, et al., 2008; Murphy & Pandis, 2009). However, in recognizing that the aging of BSOA does occur, some other modelling works (Karnezi, et al., 2018; Woody, et al., 2016; Bergström, et al., 2012; Donahue, et al., 2012a) performed some sensitivity simulations enabling this process. A more recent study focused on multi-generational aging (Jathar, et al., 2016) highlighted that SOA aging is however

probably not very important at urban-suburban scales, and suggests that adding aging reaction of SOA may be double counting SOA formation (i.e., this effect is already included in aerosol yields).
Since the literature is somewhat controversial on this issue, we decided to perform two additional runs to evaluate the sensitivity of CAMx to different aging schemes, (1) applying the current aging scheme also to BSOA (*06_vbs_bioaging*) and (2) turning off the whole aging scheme (*07_vbs_noaging*).

2.6 Summary of the simulation set

Summing up, we performed seven simulations to address different uncertain aspects of CAMx input setup, with the methods described in the previous sections. The main characteristics and the labels for all the seven runs are summarized in Table 5.

2.7 Comparison with observations

Observed concentrations of traditional air pollutants (e.g. $PM_{2.5}$, NO_x) are provided by the European database of national monitoring networks (AirBase) in Europe. AirBase is the European air quality database maintained by the EEA through its European topic center on Air pollution and Climate Change mitigation (https://www.eea.europa.eu/data-and-maps/data/aqereporting-2). We integrated AirBase dataset with data from sites managed by Italian Regional Agencies for Environmental Protection (ARPA). Only background stations (rural, suburban and urban) with an hourly data coverage higher than 75% in simulation year 2013 were chosen. Figure 1 shows the location of such measurement stations.

Table 5 - Main characteristics of the 7 sensitivity runs presented in this work

Run label	Gas-phase chem	OA-chem	Notes
00_vbs_meroni	CB05	VBS	Meroni et al. (2017) configuration
01_soap2_newbase	CB6r4	SOAP2	Revised yields for SOA production
02_vbs_newbase	CB6r4	VBS	New CAMx version, revised OM/EC
03_soap2_newivoc	CB6r4	SOAP2	Revised IVOC emissions
04_vbs_newivoc	CB6r4	VBS	Revised IVOC emissions
05_vbs_newomsv	CB6r4	VBS	Revised volatility distributions+OM_{SV}
06_vbs_bioaging	CB6r4	VBS	Enabling BSOA aging
07_vbs_noaging	CB6r4	VBS	Turning off aging scheme

For our study period, observations of organic aerosol concentrations are available for two different sites, Bologna (AMS–BO) and Ispra (ACSM–IS). Location of such sites is reported in Figure 1 with blue triangles. Ispra station is located in the Northern part of the study area and it is a rural background site affected by anthropogenic emissions (Gilardoni, et al., 2011); Bologna station is instead located in the South–Eastern part and it is representative of an urban background site. Data are available for February 2013 at Bologna site and March 2013 at Ispra site.
Details about the aerosol measurements carried out in Bologna and Ispra were already reported elsewhere (Bressi, et al., 2016; Gilardoni, et al., 2016), thus only a brief summary follows here. PM_1 concentration of nitrate, sulfate, ammonium, and OA were measured at Bologna by an Aerodyne High Resolution Time of Flight Aerosol Mass Spectrometer (HR–TOF–AMS) (DeCarlo, et al., 2006), using composition dependent collection efficiency (Middlebrook, et al., 2012) with a time resolution of 5 min. Before the sampling, particles were dried with a Nafion drier at relative humidity below 30%. Data validation was performed by comparing sulfate, nitrate, and ammonium concentration from AMS analyses with the concentration measured offline by ion chromatography on aerosol samples collected in parallel. At Ispra site, an Aerodyne Aerosol Chemical Speciation Monitor (ACSM) (Ng, et al., 2011) was used instead, based on the same operating principle but with a 30 min time resolution. Filter measurements of inorganic species are also available at Ispra site. Details about these measurements can be found in Meroni et al., (2017).

Further analysis of OA mass spectra by means of Positive Matrix Factorization (PMF) allowed the separation of ambient OA mass into different factors: hydrocarbon-like OA (HOA), biomass burning OA (BBOA) and from one (at Ispra) to three (at Bologna) types of oxygenated OA (OOA) (Bressi, et al., 2016; Gilardoni, et al., 2016). In our validation, we matched the sum of OOA factor concentrations in PM_1 with modelled SOA concentrations. HOA and BBOA are instead linked to POA deriving from anthropogenic and biomass burning sources, respectively.

3 Results

The validation of both meteorological variables and gaseous precursors for our case study is reported in Meroni et al. (2017). It is worth noting that our set of simulations differ only for OA-related features with respect to Meroni et al. (2017), and therefore a new validation of both meteorological variables and gaseous precursors was not needed. OA concentrations were validated by means of several model performance metrics. Mean Bias (MB) and Mean Fractional Bias (MFB) aim to assess the magnitude of systematic errors, Mean Fractional Error (MFE) and Root Mean Square Error (RMSE) are related to random errors whereas the index of agreement (IOA) takes into account the correlation between two timeseries. The mathematical definition of such metrics is reported in the Supplementary Material (Equations S1-S7).

The overall results of the whole set of CAMx runs in terms of organic aerosol (POA, SOA and total OA) are summarized in Figure 4. The corresponding performance metrics for total OA can be found in Table 6 and **Errore. L'origine riferimento non è stata trovata.**. A detailed discussion of each run follows in the next subsections.

Table 6 – Total organic matter (TOM) performance metrics for Meroni et al. (2017) run and the seven runs presented in this work at Bologna site (February 2013). Obs stands for the mean observed value whereas Mod represents the mean modelled one.

Run label	Obs (µg m^{-3})	Mod (µg m^{-3})	MB (µg m^{-3})	RMSE (µg m^{-3})	MFB	MFE	IOA
00_vbs_meroni	8.50	3.09	-5.41	7.21	-80.1%	85.9%	0.52
01_soap2_newbase	8.50	5.50	-3.01	5.58	-31.0%	56.4%	0.61
02_vbs_newbase	8.50	3.98	-4.52	6.43	-63.5%	72.9%	0.57
03_soap2_newivoc	8.50	6.31	-2.19	5.09	-19.8%	50.9%	0.66
04_vbs_newivoc	8.50	5.53	-2.98	5.49	-40.7%	60.0%	0.67
05_vbs_newomsv	8.50	7.19	-1.32	5.16	-18.5%	53.4%	0.73
06_vbs_bioaging	8.50	8.00	-0.50	5.19	-10.1%	52.2%	0.75
07_vbs_noaging	8.50	6.21	-2.29	5.39	-30.7%	56.9%	0.70

Table 7 – Total organic matter (TOM) performance metrics for Meroni et al. (2017) run and the seven runs presented in this work at Ispra site (March 2013). Obs stands for the mean observed value whereas Mod represents the mean modelled one.

Run label	Obs (µg m^{-3})	Mod (µg m^{-3})	MB (µg m^{-3})	RMSE (µg m^{-3})	MFB	MFE	IOA
00_vbs_meroni	14.95	—	—	—	—	—	—
01_soap2_newbase	14.95	6.50	-8.45	15.27	-58.1%	76.7%	0.45
02_vbs_newbase	14.95	4.86	-10.08	15.93	-84.1%	93.7%	0.45
03_soap2_newivoc	14.95	7.49	-7.45	14.79	-47.5%	71.0%	0.45
04_vbs_newivoc	14.95	6.63	-8.31	15.12	-64.6%	81.6%	0.46
05_vbs_newomsv	14.95	8.67	-6.28	14.60	-44.1%	73.1%	0.48
06_vbs_bioaging	14.95	9.82	-5.13	14.36	-35.0%	70.3%	0.50

07_vbs_noaging	14.95	7.33	-7.61	15.03	-56.4%	78.8%	0.46

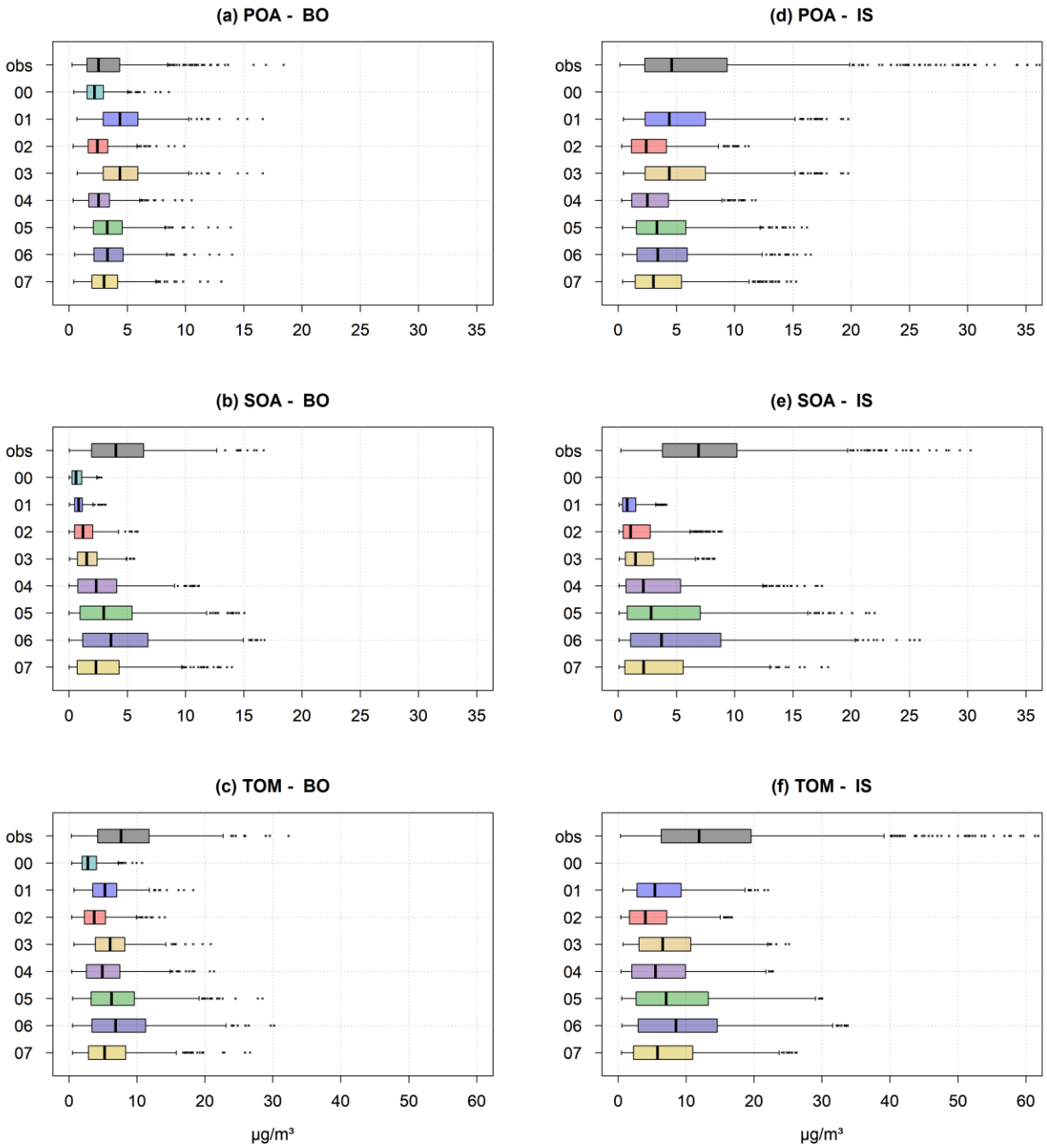

Figure 4 - Distribution of hourly POA, SOA and TOM concentrations across the whole set of CAMx runs for (a–c) Bologna site and (d–f) Ispra site. The bottom and top of the box represent the lower and upper quartiles, respectively, and the band in the middle of the box is the median value of the distribution. The whiskers extend to the most extreme data point which is no more than 1.5 times the interquartile range from the box.

3.1 The base case

The few changes with respect to Meroni et al. (2017) work (i.e. new CAMx version, CB6r4 instead of CB05 and other minor upgrades, described in Section 2.2) lead to a non-negligible variation in OA levels results. Total Organic Matter (TOM) is generally better predicted at Bologna site by the new base case

(*02_vbs_newbase*) compared to the run described in Meroni et al. (2017) (*00_vbs_meroni*), although a strong underestimation – especially for SOA concentrations (3.2 times on average) – is still present (

Figure 5a). Mean observed TOM at Bologna site is 8.50 µg m^{-3}, whereas mean modelled TOM is 3.98 µg m^{-3} and 3.09 µg m^{-3}, for the new base case and Meroni et al. (2017) run, respectively. TOM Mean Bias (MB) is therefore reduced from -5.41 µg m^{-3} to -4.52 µg m^{-3} (mean fractional bias from -80.1% to -63.5%). Index of Agreement (IOA) increases accordingly (from 0.52 to 0.57). This enhancement in model performances is mainly due to new speciation profiles (which are in favor of higher OM/EC ratios, Table 1) and the new code of CAMx, which includes a major revision to the secondary organic aerosol chemistry/partitioning algorithm (both SOAP and VBS). As Meroni et al. (2017) run was performed only for February 2013, no comparison between the new base case and *00_vbs_meroni* is possible for Ispra site, in which observed data refer to March 2013. Nonetheless, a severe underestimation of TOM and its fractions is found for our new base case at Ispra site (

Figure 5b). SOA mean concentration is underestimated by ~4 times (as it was for Bologna site) for the VBS simulation, with a mean bias of -5.88 µg m^{-3}. In contrast to Bologna simulation, we found a significant underestimation in POA mean concentration (2.4 times) as well.

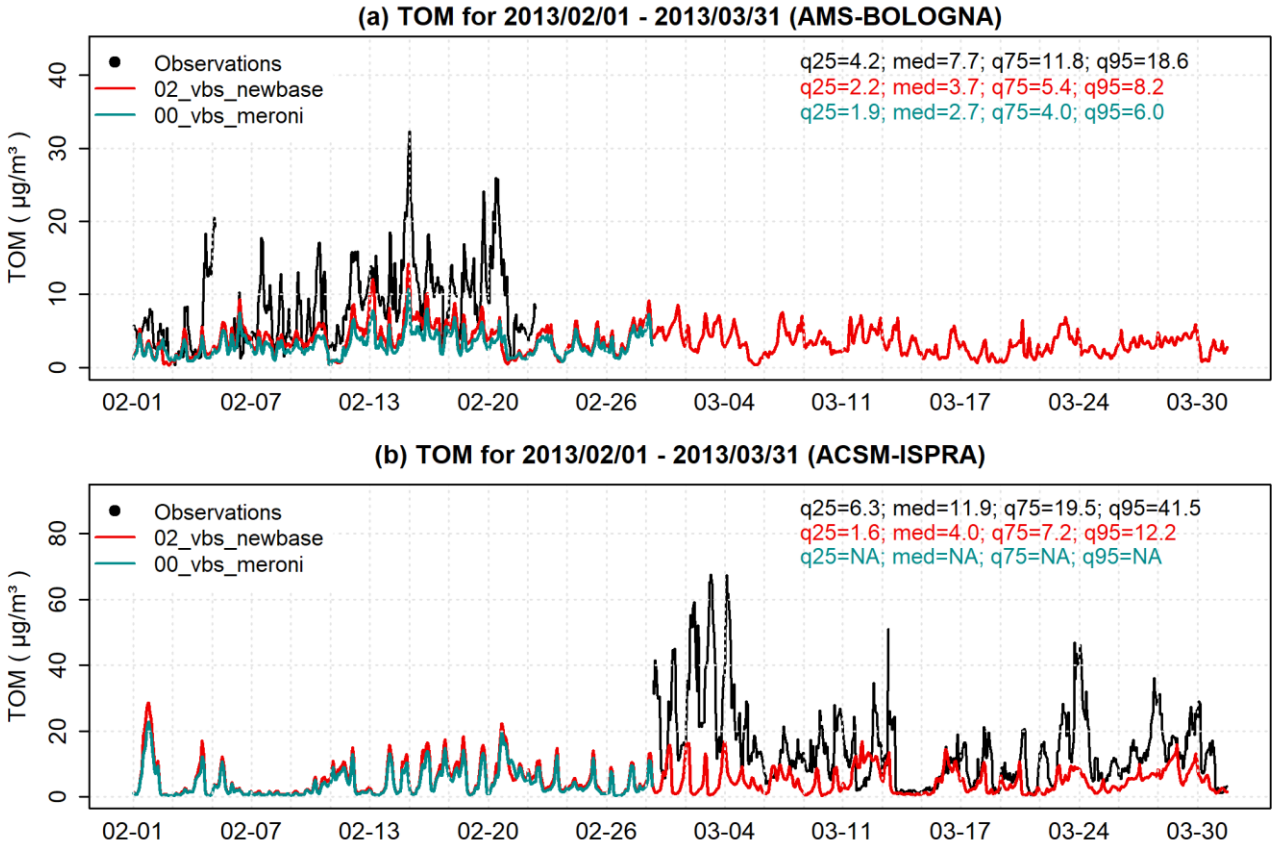

Figure 5 - Comparison between the new VBS base case and Meroni et al. (2017) run for TOM at (a) Bologna site and (b) Ispra site. The new base case is labelled as 02_vbs_newbase (red) and the run of Meroni et al. (2017) is labelled as 00_vbs_meroni (cyan). Statistics are computed with pairwise–complete observations.

This is confirmed by the analysis of POA fractions (i.e. HOA and BBOA) presented in the Supplementary Material (Figure S1 and Figure S2). The clear underestimation of BBOA fraction might be due to missing SVOC emission from BB (as underlined by Denier van der Gon et al., 2015) and to an incorrect spatial distribution of such emissions. As a matter of fact, mean modelled BBOA concentration in Ispra and in Bologna are similar (2.59 and 2.08 µg m^{-3}, respectively) whereas the observed ones are much more different (6.36 and 2.38 µg m^{-3}, respectively). Such difference in BBOA measurements might be explained by the location of the two stations. Ispra station is a rural background site strongly affected by anthropogenic emissions (Henne et al., 2010) – where wood combustion in the residential sector is an important source of atmospheric aerosol – while Bologna station is an urban one, where residential heating is mainly accomplished by natural gas burning. However, this large spatial gradient is not well captured by CAMx, likely because of

an inaccurate spatialization of BBOA emissions. HOA underestimation is instead related to an incorrect representation of peaks magnitude for both Bologna and Ispra site, as clear from the daily profiles of Figure 6. Finally, SOAP2 run (*01_soap2_newbase*) leads to a slightly better agreement for TOM prediction compared to the VBS run, at both Bologna and Ispra sites. At Bologna site, MB shifts from -4.52 µg m^{-3} in the VBS run to -3.01 µg m^{-3} in the SOAP2 run. RMSE decreases accordingly, from 6.43 µg m^{-3} to 5.58 µg m^{-3}. However, this improvement in TOM levels is associated with a degradation in both SOA and POA performances, i.e. error compensation gives overall a better result in terms of concentration, but not in terms of SOA and POA fractions (Figure 7).

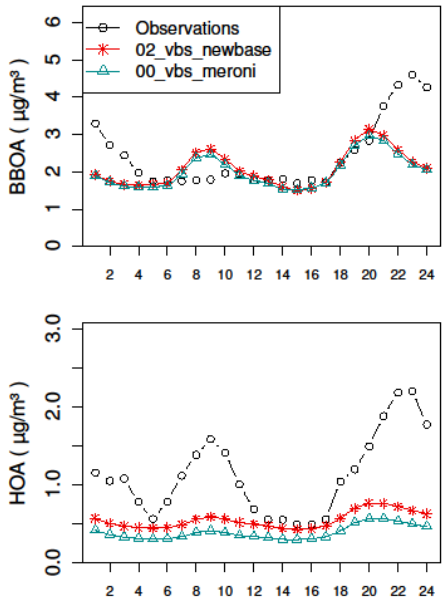

Figure 6 - Comparison of daily profiles of BBOA and HOA between the new VBS base case and Meroni et al. (2017) run at Bologna site. The new base case is labelled as *02_vbs_newbase* (red) and the run of Meroni et al. (2017) is labelled as *00_vbs_meroni* (cyan).

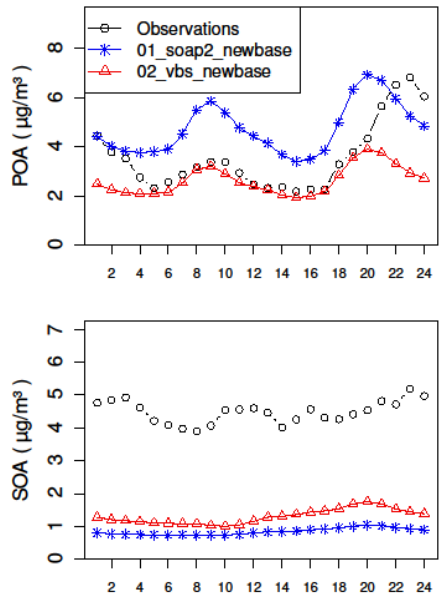

Figure 7 - Comparison of daily profiles of POA and SOA calculated with SOAP2 and VBS algorithms at Bologna site. The SOAP2 run (blue) is labelled as *01_soap2_newbase* and the VBS one (red) is labelled as *02_vbs_newbase*.

3.2 New IVOC parametrization

We expect that revisions in IVOC emissions parametrizations (runs labelled as *03_soap2_newivoc* and *04_vbs_newivoc*) should significantly affect the secondary fraction of organic aerosol. Nevertheless, minor changes might be observed on POA as well, since a variation in SOA concentration leads to a different OA total mass, thus influencing the overall partitioning of POA.

We found out a considerable improvement for the modelled SOA concentrations in *04_vbs_newivoc*, compared to the VBS base case (Figure 8) at Bologna site. SOA mean bias is reduced from -3.07 µg m^{-3} to -1.62 µg m^{-3} (MFB from -98.7% to -53.6%), and IOA increases from 0.53 to 0.70 (Table S4). POA mean concentration slightly increases as a consequence of SOA increase (MB from -0.92 µg m^{-3} to -0.81 µg m^{-3}, Table S1).

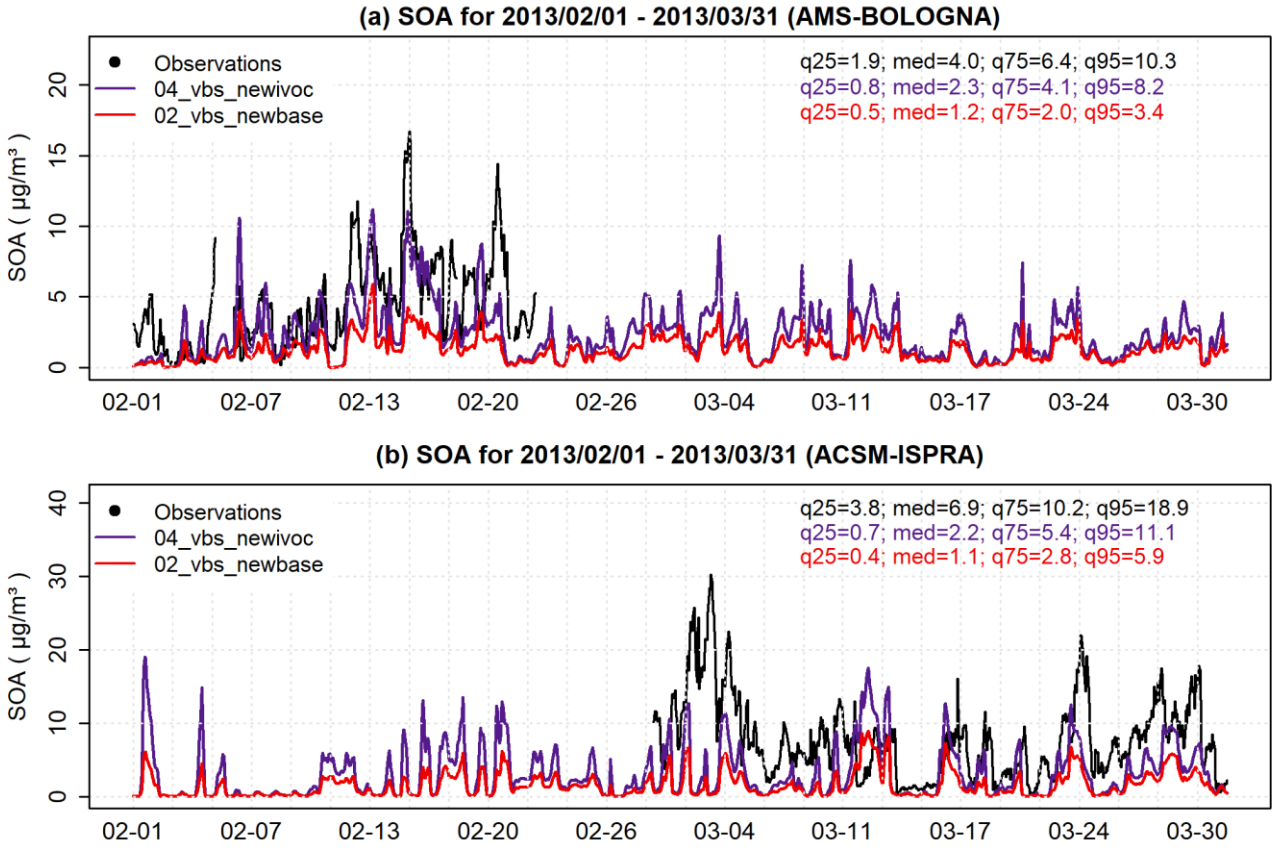

Figure 8 - Effect of the revision in IVOC emissions (*04_vbs_newivoc*, purple) on the new VBS base case run (*02_vbs_newbase*, red) for SOA at (a) Bologna site and (b) Ispra site. Statistics are computed with pairwise–complete observations.

Enhancement of TOM performances (IOA from 0.57 to 0.67, Mean Fractional Error from 72.9% to 60.0%, Table 6) are therefore mainly due to SOA improvement. This much better agreement (especially for SOA) suggests that updated IVOC emissions parametrizations are crucial for a better prediction of organic aerosol concentrations. Similar improvements are found for Ispra site (Figure 8), even though the SOA performance metrics clearly indicate overall poorer results (IOA from 0.47 to 0.50, MB from -5.88 to -4.24 µg m-3, Table S8).

Applying the new IVOC parametrizations to the same base case with SOAP2 algorithm (*03_soap2_newivoc*) leads again to worse results in terms of both POA and SOA concentrations compared to the equivalent VBS run (*04_vbs_newivoc*) and highlights therefore the limits of SOAP2 compared to VBS (Figure S3). The increased yields of SOAP2 and the new IVOC parametrizations are not capable of correctly reproducing SOA observed concentrations, whereas the VBS approach (with the same amount of IVOC emissions) provides much better results. The comparison between *03_soap2_newivoc* and *04_vbs_newivoc* confirms that revised IVOC emissions can help filling the gap between modelled and observed SOA as long as VBS algorithm is applied (Figure S3 and Table S4).

3.3 New volatility distribution and OM_{SV} estimates

Run labelled *04_vbs_newivoc* addressed the issue of IVOC emission parametrization, whereas we implicitly set OM_{SV} emissions (organic matter in the semi–volatile range) equal to POA emissions. Further improvements in OA levels prediction can be obtained by applying new volatility distributions and new OM_{SV} emissions according to the methods explained in Section 2.4. These revisions entail three main differences between *05_vbs_newomsv* and *04_vbs_newivoc*: (i) updated volatility distributions applied to GV and DV emissions, (ii) increased total emissions of OM_{SV} for GV, DV and BB and (iii) increased IVOC emissions from biomass burning (IVOB) as IVOB are scaled on OM_{SV}.

A very good agreement between modelled and observed TOM is obtained in *05_vbs_newomsv* (Figure 9). At Bologna site, mean bias for TOM is reduced from -2.98 µg m^{-3} in the previous run (*04_vbs_newivoc*) to -1.32 µg m^{-3} (MFB from -40.7% to -18.5%), and IOA increases from 0.67 to 0.73 (Table 6).

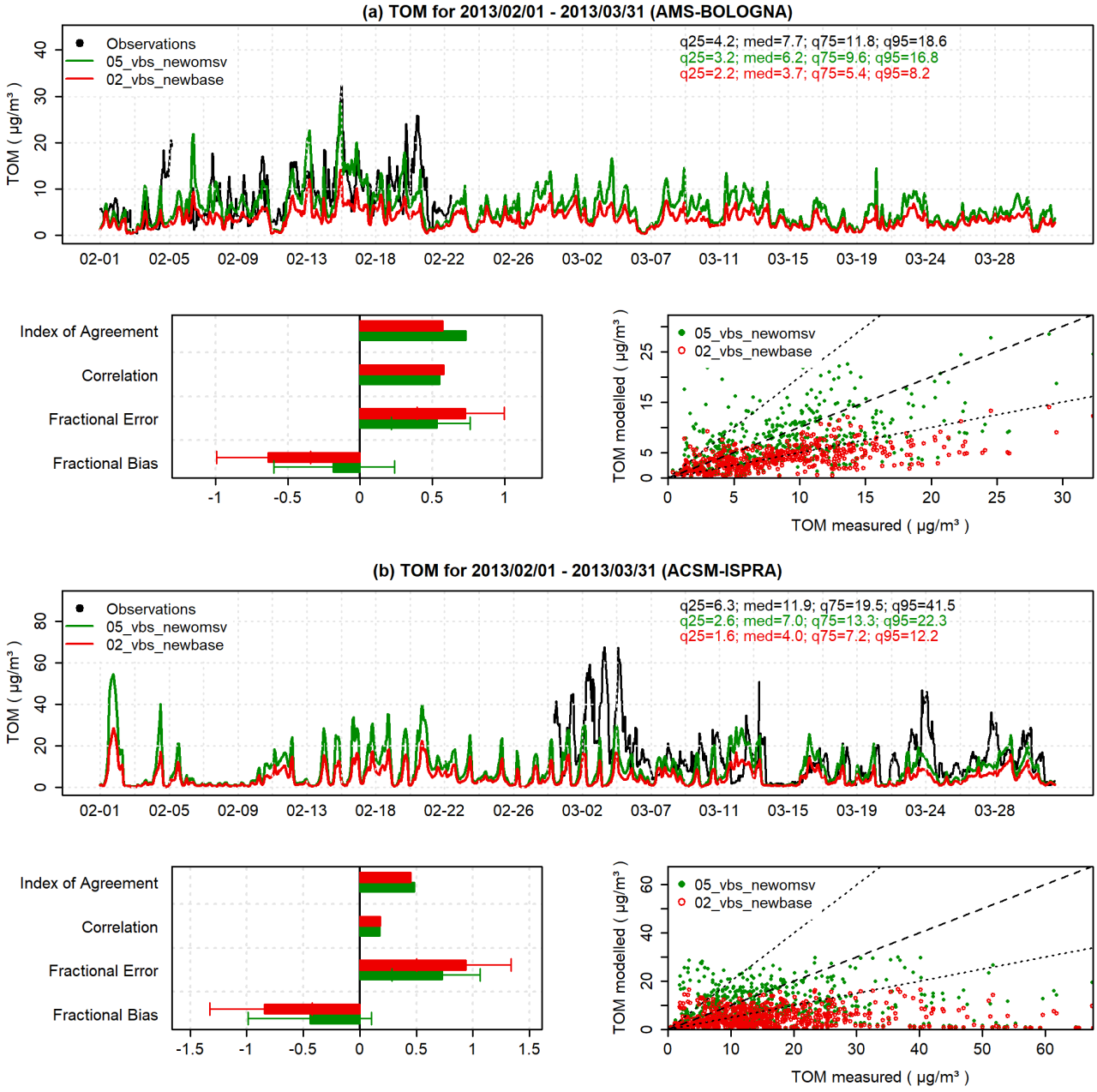

Figure 9 - Effect of the revision in OM_{SV} emissions and volatility distributions (*05_vbs_newomsv*, green) on the new base case run (*02_vbs_newbase*, red) for TOM at (a) Bologna site and (b) Ispra site. Statistics are computed with pairwise–complete observations.

Again, this performance enhancement is associated with a significant improvement in both SOA and POA prediction, due to the new volatility distribution and new OM_{SV} revisions. IOA for SOA increases up to 0.75

and mean bias decreases to -0.76 μg m^{-3}, which is a remarkable result compared to the base case (IOA = 0.53, MB = -3.07 μg m^{-3}, Table S4). It should be noted that SOA mean concentration increases compared to the previous run, for two main reasons: (i) increased material in the semi-volatile range which can form SOA and (ii) increased IVOC emissions from biomass burning as IVOC are scaled on OM_{SV} emissions.

3.4 Model sensitivity to aging schemes

We performed two additional runs (based on *05_vbs_newomsv*) to assess the sensitivity of CAMx to different aging schemes, (i) applying the current aging scheme to BSOA as well (*06_vbs_bioaging*) and (ii) turning off the whole aging scheme (*07_vbs_noaging*). The results of the two simulations are summarized in Figure 4. As expected, enabling aging of BSOA helps in closing the gap between observed and modelled SOA. At Bologna site, mean bias of SOA decreases from -0.76 μg m^{-3} (in *05_vbs_newomsv*) to ~0, even though this is associated with a slight increase in RMSE (from 3.13 μg m^{-3} in *05_vbs_newomsv* to 3.34 μg m^{-3} when enabling aging of BSOA). IOA remains almost unchanged. The results of the last simulation (07_vbs_noaging) suggests that the addition of aging reactions leads to a little improvement for wintertime TOM prediction. As a matter of fact, when removing all aging reactions MB and RMSE of TOM increases (MB from -1.32 μg m^{-3} to -2.29 μg m^{-3}, RMSE from 5.16 μg m^{-3} to 5.39 μg m^{-3}) and IOA decreases accordingly (from 0.73 to 0.70).
At Ispra site, SOA mean bias decreases from -3.30 μg m^{-3} to -2.21 μg m^{-3}, and IOA increases accordingly (0.52 to 0.55) when moving from *05_vbs_newomsv* to *06_vbs_bioaging*. The modelled aging of BSOA produces a non-negligible amount of SOA in Ispra station during March, on average 1.09 μg m^{-3}. Turning off the whole aging scheme leads to a considerable performance worsening for SOA prediction, as aging processes implemented in *05_vbs_newomsv* are responsible for ~1 μg m^{-3} of SOA, which is ~15% of total observed SOA.

3.5 Meteorological influence on organic aerosol levels

Meteorology plays a crucial role in determining OA levels, especially in the Po Valley area. Frequent stagnation events and persistent conditions of atmospheric stability are mainly responsible for the high OA concentrations observed in both Bologna and Ispra site, which are respectively ~3 and ~5 times larger than the average OA concentration across 11 sites in Europe (Ciarelli, et al., 2017a). Consequently, modelling the correct meteorological conditions is essential to properly reproduce OA levels.
For Bologna site, two clear anticorrelated periods in TOM concentrations are found during February (around 6^{th}-7^{th} and 19^{th}-20^{th} February, Figure 9). Both those examples are likely linked to an erroneous meteorological simulation (Figure S4 and Figure S5), as we found out that the meteorological model completely misses a precipitation event (6^{th}–7^{th} February) and a strong Föhn wind event (19^{th}–20^{th} February), which might explain the non–observed peaks occurring during those days.
At Ispra site, fairly good performances are achieved from March 6 to the end of the month (Figure 9). The first part of March (1^{st}–6^{h} March) shows instead an almost anti-correlated behavior for TOM, meaning that CAMx misses the first peaks for both TOM and SOA. This anticorrelated period negatively affects the overall validation statistics which turn out to be worse compared to Bologna site. A strong underestimation at the beginning of the month has been found out also for other PM fractions (e.g. nitrate, Figure S6) and other gaseous precursors, like nitrogen oxides (Figure S7). Hence, we further analyzed vertical temperature profiles to assess whether the meteorological model WRF is able to reproduce the stability condition which was clearly in place during those days. Results of such analysis are presented in Figure 10 for four exemplifying days, and they show a general incorrect representation of the temperature inversions layers which were in place during those days. Even though this analysis is limited to one station (Milano Linate) which is 63.9km away from Ispra site, we can reasonably suppose that OA underestimation in the first period is to some extent related to a misrepresentation of the atmospheric stability condition.

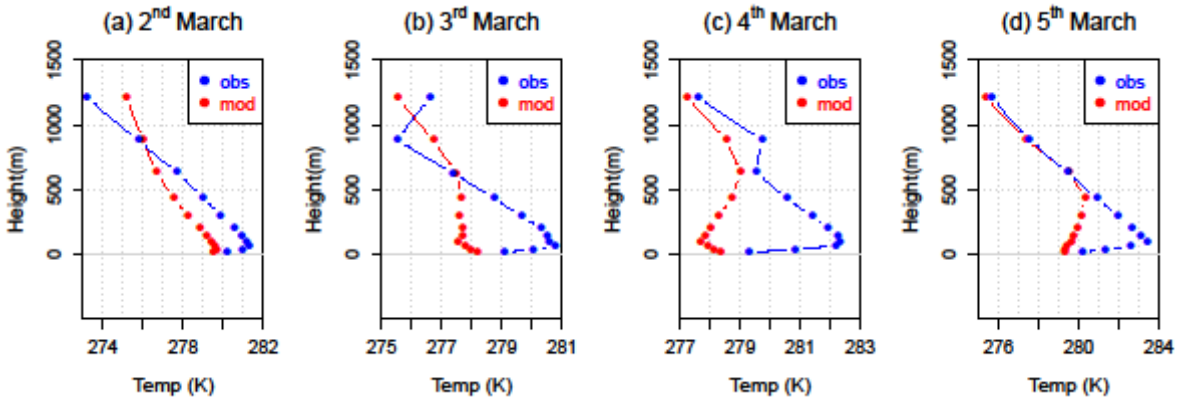

Figure 10 - Modelled (red) and observed (blue) vertical temperature profiles for four different days at 00 CET.

The effect of erroneous meteorological modelling, as well as the importance of meteorology in the Po Valley area, is further illustrated in Figure 11 for TOM. The stagnation event during 1st-6th March leads to exceptionally high concentrations of TOM, which are not captured by the model. However, when meteorological conditions are well reproduced (7th-31st March), satisfactory performances are achieved, especially when taking into account S/IVOC and volatility distributions revisions. A more complete comparison of the model performance evaluation between these two periods is presented in the supplementary material (Figure S8-S9 and Table S9).

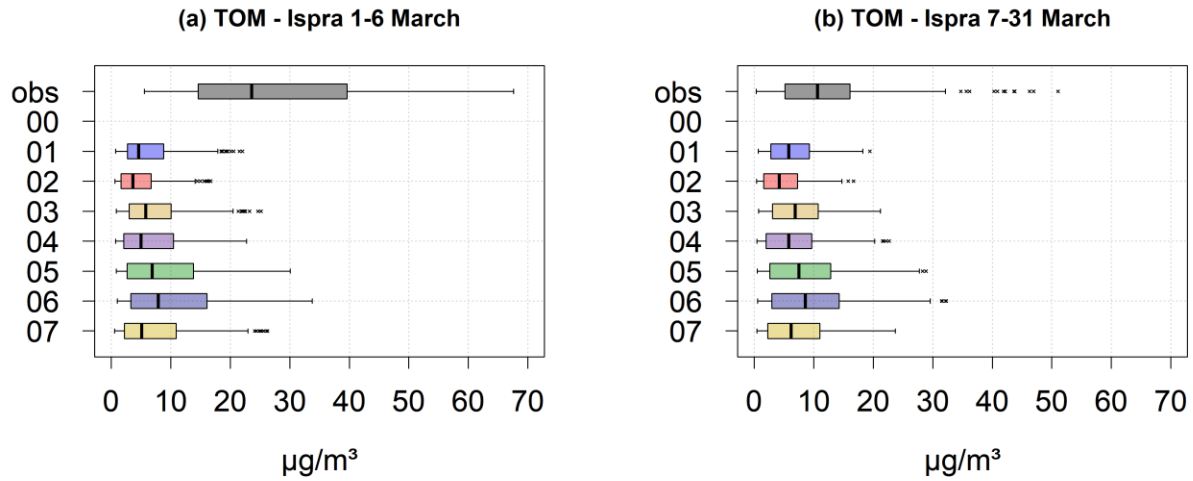

Figure 11 - Distribution of hourly POA, SOA and TOM concentrations across the whole set of CAMx runs for (a) Ispra site during 1st-6th March and (b) Ispra site during 7h-31st March. The bottom and top of the box represent the lower and upper quartiles, respectively, and the band in the middle of the box is the median value of the distribution. The whiskers extend to the most extreme data point which is no more than 1.5 times the interquartile range from the box.

4 Discussion

Table 6 and **Errore. L'origine riferimento non è stata trovata.** summarize the main performance metrics for TOM at Bologna and Ispra sites, respectively. The same validation indices for each fraction of OA (i.e. POA, SOA, BBOA and HOA) are reported in the supplementary material (Table S1 to Table S8). At Bologna urban site, mean fractional bias for TOM ranges from -80.1% in the worst case run (*00_vbs_meroni*) to -10.1% in the best one (*06_vbs_bioaging*) and IOA from 0.52 to 0.75. Notable improvements, though with overall poorer metrics, are found for Ispra site, where MFB ranges from -84.1% to -35.0% and IOA from 0.45 to 0.50. Underestimation of total organic matter remains still relevant in Ispra, although our revisions do significantly improve model performances. It should be noted that a much higher TOM is observed in Ispra with respect to

Bologna (15.0 ± 12.5 µg m^{-3} and 8.50 ± 5.51 µg m^{-3}, mean ± standard deviation, respectively), which is to some extent surprising and confirms the importance of residential wood heating in OA concentrations.
Comparable results were found in other European modelling studies in which similar revisions in S/IVOC parametrizations and volatility distributions were applied (Chrit et al., 2018; Ciarelli et al., 2017a). It is worth noting that these results were obtained in very different conditions, with the observed OA mean concentration being in the range 2-3 µg m^{-3} (Chrit et al., 2018; Ciarelli et al., 2017a) compared to 15.0 and 8.5 µg m^{-3} observed in Ispra and Bologna, respectively.
Despite the improvements, both the timeseries of Figure 9 and the daily profiles of Figure 12 show that there are still some issues to be tackled.

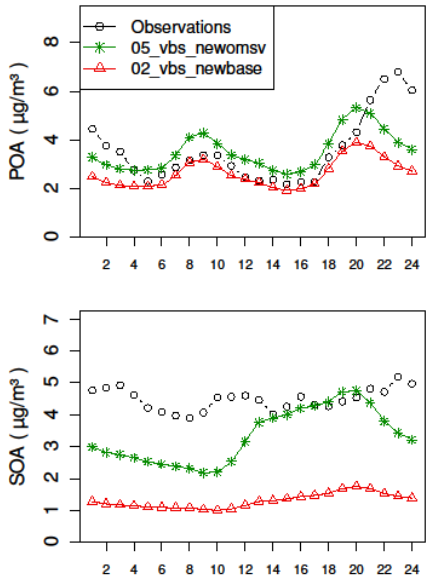

Figure 12 - Daily profiles of POA and SOA concentrations at Bologna site for two different runs: 05_vbs_newomsv (green) includes all the revisions in S/IVOC and volatility distributions whereas 02_vbs_newbase (red) is the new VBS base case presented in this work.

BBOA and HOA (which sum up to total POA) suffer from the two main limitations pointed out in Meroni et al. (2017) though to a minor extent. BBOA is underestimated during night–time across the different simulations, and this may depend on an inaccurate representation of vertical dispersion (i.e. partial overestimation of the planetary boundary layer height). Moreover, modelled BBOA daily profile present two peaks, at 8am and 8pm (Figure 6), which is somehow counterintuitive as BBOA derive mostly from biomass burning emissions. This is linked to improper temporal profiles applied in the emissions preparation model, because biomass burning activities fall under the wider "Non-industrial combustion plants" sector. Given the importance of BBOA concentrations with the respect to total OA, a more refined and specific temporal profile for BB emissions could be developed in future studies. HOA concentrations face instead a systematic underestimation of the rush–hour peaks, even though our revisions improve the model performances compared to Meroni et al. (2017) run. This might be due to the relatively low spatial resolution used in CAMx (5km), especially for the urban site of Bologna where the influence of local traffic may be relevant. An integrated modelling approach, using also a nested Lagrangian local scale model as done in Pepe et al. (2016), could enhance HOA peaks prediction.
Observed SOA daily profile is instead rather flat, as it was also for other European studies (Ots, et al., 2016; Fountoukis, et al., 2014). Model results show however a stronger diurnal cycle peaking in the late afternoon (Figure 11), indicating that vertical dispersion during night–time is probably misrepresented, as modelled SOA concentrations (and other primary pollutants, e.g. HOA and BBOA) decline after 8pm whereas the observations show further accumulation. However, the discrepancies in SOA daily profiles might also be partially due to an underestimation of the importance of aging processes which can flatten the SOA daily profile.

The relative contribution of POA and SOA to total organic matter is much better reconstructed by VBS scheme compared to the traditional SOAP algorithm, even when the revised yields are applied (the so–called SOAP2 in CAMx): the non–volatile treatment of POA leads to a general overestimation of POA concentrations associated with a strong underestimation in SOA concentrations. Within the VBS framework, POA is instead allowed to evaporate (depending on the partitioning), and vapors can be oxidized in the atmosphere (becoming less volatile) and re-condense back to SOA. The relevance of both the aging processes and the non–volatile treatment of POA suggest therefore that VBS algorithm should be employed as the state-of-the-art scheme for OA calculation in CTM, as done in the latest modelling works (Ciarelli, et al., 2017a; Jathar, et al., 2017).

As for the contributions of different emission sources to total OA, we found out that biomass burning activities are a major source of organic matter during winter time, both in the observations and in the modelling results. This finding is coherent with other European studies (Glasius, et al., 2018; Ciarelli, et al., 2017a; Bergström, et al., 2012), but in contrast with some American works (Jathar, et al., 2017; Shrivastava, et al., 2011) where more relevance is given to mobile sources emissions. At Ispra site, for *05_vbs_newomsv*, modelled primary organic aerosol is 48.3% (on average) of the total organic matter, whereas secondary matter contributes for 51.7%. The secondary contribution is slightly lower compared to the findings of Ciarelli et al. (2017a), in which the secondary fraction was accounting for 62% of total organic matter as an average between 11 sites across Europe. The difference is most likely due to the high emissions of POA coming from residential wood heating in the Ispra area, which increases the contribution of primary matter compared the average of Ciarelli et al. (2017a). As expected, modelled POA is predominantly composed by biomass–burning particles, which account for 89.1% of total POA, reflecting the findings for the total emission budget (Table 4). Observations show a similar POA/TOM and SOA/TOM ratios (47.9% and 52.1% on average, respectively) as well as the BBOA/POA ratio (89.0%). Similar figures are found for the urban Bologna site, except for the contribution of BBOA to total POA: the modelled BBOA/POA value is similar (83.6%) whereas the observed one is much smaller (68.8%), highlighting that for this urban site HOA concentrations are underestimated, as already mentioned.

Finally, we showed that enabling aging of BSOA (SOA deriving from biomass burning and biogenic precursor) would help to close the gap between the observations and the model in terms of SOA, which is in contrast to some other American studies (Lane, et al., 2008; Murphy & Pandis, 2009). However, this performance improvement does not directly imply that missing BSOA aging processes is certainly responsible for SOA underestimation. Results might be improved for the wrong reasons as a lot of other assumptions are required in the VBS scheme. For instance, increasing SOA yields from VOC precursors would lead to a similar improvement in model performances, but at the moment we cannot really distinguish whether SOA underestimation is due to low SOA yields or missing aging of BSOA. The most reasonable option is probably to keep the default yields and aging scheme in CAMx, as VBS yields are based on chamber data which allows further oxidation (aging) of the first-generation products (Koo, et al., 2014). Therefore, application of these yields together with a different aging scheme might lead to a conceptually incorrect representation of SOA formation (i.e. double counting of SOA formation). Further work is necessary to better constrain the aging scheme, even though here we provide evidence that aging of BSOA would help in getting a more realistic SOA representation at both AMS and ACMS sites. A summertime simulation could be helpful in further understanding aging schemes impact on summertime TOM concentrations.

5 Conclusions

We presented a high–resolution (5km) set of new simulations performed with CAMx v6.40 over the Po Valley area (Northern Italy), aimed to enhance OA levels prediction and to gain insight into the sensitivity of CAMx to different uncertain features of the input setup. In particular, we investigated the role of volatility distributions of organics emissions, S/IVOC emissions parametrizations, SOA yields from S/IVOC precursors and different aging schemes by exploiting the latest experimental information available in the scientific literature. Model results were validated against two OA–specific datasets, available for both an urban site (Bologna, February

2013) and a rural one (Ispra, March 2013). We may summarize the main conclusions stemming from our analysis as follows:

- Overall, we found a considerable performance improvement on modelled OA concentrations when applying new S/IVOC emission estimates and the new volatility distributions. However, despite a great performance enhancement, SOA concentrations remain the most underestimated among the different OA components, especially for Ispra site. Further analysis on SOA source (i.e. anthropogenic, biogenic and biomass–burning) and SOA aging, also based on the analysis of oxidation state (as done in Chrit et al., 2018) could provide a helpful insight for future enhancements in SOA prediction. Of course, very detailed measurements of SOA would be required for such analyses, but they could give indications on (i) which SOA source is more responsible of SOA underestimation, (ii) how much the development of stagnation conditions can influence the accumulation of pollutants and (iii) to what extent our current aging scheme is reproducing the actual aging processes of source–specific SOA and therefore its tendency to remain in the atmosphere, particularly during stagnation conditions.
- CAMx proved to be very sensitive to IVOC emissions. Updated parametrizations of these compounds from the most recent experimental studies significantly contribute in mitigating the large underestimation of SOA which was present in the traditional algorithm. However, a thorough literature review underlined a large variability between different estimates of source–specific IVOC emissions from different authors. Even though the parametrizations identified in this work seem to provide satisfactory results, further experimental work (especially in Europe) to better constrain IVOC emissions is suggested.
- We argue that organic matter in the semi-volatile range is most likely underestimated in the current emissions inventories. We gave evidence of this point for diesel, gasoline and biomass burning emissions. A correct representation of OM_{SV} in the official emission inventories – as well as up-to-date volatility distributions – appear to be very relevant in improving model performances.
- A correct meteorological input is fundamental in accurately reproducing organic aerosol concentrations for the Po Valley area, as pointed out in Section 3.5. By analyzing also the meteorological simulation and the behavior of other pollutants (e.g. NO_x, elemental carbon and inorganic ions), we found out that most of the periods characterized by inaccurate TOM concentrations are linked to an incorrect reconstruction of the meteorological conditions (e.g. mixing layer evolution, precipitation and strong wind events).
- Model results did not show a very pronounced sensitivity to aging processes, due to the low photochemical activity typically observed during winter-time. However, we give evidence that enabling aging processes for biomass burning related SOA, which is by default disabled in CAMx v6.40, can help in closing the gap between modelled and observed SOA concentrations.

Acknowledgements. RSE contribution was funded by the Research Fund for the Italian Electrical System under the Contract Agreement between RSE S.p.A. and the Ministry of Economic Development - General Directorate for Nuclear Energy, Renewable Energy and Energy Efficiency in compliance with the Decree of March 8, 2006. The aerosol characterization in Bologna was funded by Regione Emilia Romagna as part of the "Supersito" project (DRG of Emilia-Romagna Region 428/10 and 1971/13). Authors are very grateful to Regional Environmental agencies of Lombardia, Piemonte, Veneto and Emilia–Romagna for kindly providing meteorological and air quality observations. Authors wish also to thank JRC (Ispra, Italy) that through EBAS platform shares observed data collected at Ispra (Italy) EMEP site. Authors would also thank RAMBOLL–ENVIRON that shares CAMx code for free and especially Dr. G. Yarwood and dr. B. Koo for a fruitful discussion about the design of the modelling experiments. Authors are also thankful to Dr. H. Denier van der Gon from TNO for providing useful information about residential wood combustion emissions of organic aerosol.

References

Barmpadimos, I., Keller, J., Oderbolz, D., Hueglin, C., & Prévôt, A. S. (2012). One decade of parallel fine ($PM_{2.5}$) and coarse (PM_{10}–$PM_{2.5}$) particulate matter measurements in Europe: trends and variability. *Atmospheric Chemistry and Physics, 12*, 3189-3203.

Bergström, R., Denier van der Gon, H. A., Prévôt, A. S., Yttri, K. E., & Simpson, D. (2012). Modelling of organic aerosols over Europe (2002-2007) using a volatility basis set (VBS) framework: application of different assumptions regarding the formation of secondary organic aerosol. *Atmospheric Chemistry and Physics, 12*, 8499-8527.

Bressi, M., Cavalli, F., Belis, C. A., Putaud, J.-P., Fröhlich, R., Martins dos Santos, S., et al. (2016). Variations in the chemical composition of the submicron aerosol and in the sources of the organic fraction at a regional background site of the Po Valley (Italy). *Atmospheric Chemistry and Physics, 16*, 12875-12896.

Caserini, S., Galante, S., Ozgen, S., Cucco, S., Gregorio, K., & Moretti, M. (2013). A methodology for elemental and organic carbon emission inventory and results for Lombardy region, Italy. *Science of The Total Environment, 450-451*, 22-30.

Caserini, S., Giani, P., Cacciamani, C., Ozgen, S., & Lonati, G. (2017). Influence of climate change on the frequency of daytime temperature inversions and stagnation events in the Po Valley: historical trend and future projections. *Atmospheric Research, 184*, 15-23.

Chrit, M., Sartelet, K., Sciare, J., Majdi, M., Nicolas, J., Petit, J.-E., & Dulac, F. (2018). Modeling organic aerosol concentrations and properties during winter 2014 in the northwestern Mediterranean region. *Atmospheric Chemistry and Physics, 18*(24), 18079-18100.

Ciarelli, G., Aksoyoglu, S., Crippa, M., Jimenez, J.-L., Nemitz, E., Sellegri, K., et al. (2016). Evaluation of European air quality modelled by CAMx including the volatility basis set scheme. *Atmospheric Chemistry and Physics, 16*, 10313-10332.

Ciarelli, G., Aksoyoglu, S., El Haddad, I., Bruns, E. A., Crippa, M., Poulain, L., et al. (2017a). Modelling winter organic aerosol at the European scale with CAMx: evaluation and source apportionment with a VBS parameterization based on novel wood burning smog chamber experiments. *Atmospheric Chemistry and Physics, 17*, 7653-7669.

Ciarelli, G., El Haddad, I., Bruns, E., Aksoyoglu, S., Möhler, O., Baltensperger, U., et al. (2017b). Constraining a hybrid volatility basis-set model for aging of wood-burning emissions using smog chamber experiments: a box-model study based on the VBS scheme of the CAMx model (v5.40). *Geoscientific Model Development, 10*, 2303-2320.

DeCarlo, P. F., Kimmel, J. R., Trimborn, A., Northway, M. J., Jayne, J. T., Aiken, A. C., et al. (2006). Field-Deployable, High-Resolution, Time-of-Flight Aerosol Mass Spectrometer. *Analytical Chemistry, 78*, 8281-8289.

Denier van der Gon, H. A., Bergström, R., Fountoukis, C., Johansson, C., Pandis, S. N., Simpson, D., et al. (2015). Particulate emissions from residential wood combustion in Europe – revised estimates and an evaluation. *Atmospheric Chemistry and Physics, 15*, 6503-6519.

Donahue, N. M., Epstein, S. A., Pandis, S. N., & Robinson, A. L. (2011). A two-dimensional volatility basis set: 1. organic-aerosol mixing thermodynamics. *Atmospheric Chemistry and Physics, 11*, 3303-3318.

Donahue, N. M., Henry, K. M., Mentel, T. F., Kiendler-Scharr, A., Spindler, C., Bohn, B., et al. (2012a). Aging of biogenic secondary organic aerosol via gas-phase OH radical reactions. *Proceedings of the National Academy of Sciences, 109*, 13503-13508.

Donahue, N. M., Kroll, J. H., Pandis, S. N., & Robinson, A. L. (2012b). A two-dimensional volatility basis set – Part 2: Diagnostics of organic-aerosol evolution. *Atmospheric Chemistry and Physics, 12*, 615-634.

Donahue, N. M., Robinson, A. L., Stanier, C. O., & Pandis, S. N. (2006). Coupled Partitioning, Dilution, and Chemical Aging of Semivolatile Organics. *Environmental Science & Technology, 40*, 2635-2643.

EEA. (2017). *Air Quality in Europe - 2017 Report.* EEA Report No 13/2017, European Environment Agency.

EMEP. (2016). *EMEP/EEA air pollutant emission inventory guidebook.* EEA Report No 21/2016, European Environment Agency.

ENVIRON. (2016). *CAMx (Comprehensive Air Quality Model with extensions) User's Guide Version 6.40.* ENVIRON International Corporation, Novato, CA.

EPA. (2005). *Conversion Factors for Hydrocarbon Emission Components.* EPA420-R-05-015, December 2005, NR-002c .

Ferrero, L., Riccio, A., Perrone, M. G., Sangiorgi, G., Ferrini, B. S., & Bolzacchini, E. (2011). Mixing height determination by tethered balloon-based particle soundings and modeling simulations. *Atmospheric Research, 102*, 145-156.

Fountoukis, C., Megaritis, A. G., Skyllakou, K., Charalampidis, P. E., Denier van der Gon, H. A., Crippa, M., et al. (2016). Simulating the formation of carbonaceous aerosol in a European Megacity (Paris) during the MEGAPOLI summerand winter campaigns. *Atmospheric Chemistry and Physics, 16*, 3727-3741.

Fountoukis, C., Megaritis, A. G., Skyllakou, K., Charalampidis, P. E., Pilinis, C., Denier van der Gon, H. A., et al. (2014). Organic aerosol concentration and composition over Europe: insights from comparison of regional model predictions with aerosol mass spectrometer factor analysis. *Atmospheric Chemistry and Physics, 14*, 9061-9076.

Fountoukis, C., Racherla, P. N., Denier van der Gon, H. A., Polymeneas, P., Charalampidis, P. E., Pilinis, C., et al. (2011). Evaluation of a three-dimensional chemical transport model (PMCAMx) in the European domain during the EUCAARI May 2008 campaign. *Atmospheric Chemistry and Physics, 11*, 10331-10347.

Fuzzi, S., Baltensperger, U., Carslaw, K., Decesari, S., Denier van der Gon, H., Facchini, M. C., et al. (2015). Particulate matter, air quality and climate: lessons learned and future needs. *Atmospheric Chemistry and Physics, 15*, 8217-8299.

Gabele, P. (1997). Exhaust Emissions from Four-Stroke Lawn Mower Engines. *Journal of the Air & Waste Management Association, 47*, 945-952.

Gilardoni, S., Massoli, P., Paglione, M., Giulianelli, L., Carbone, C., Rinaldi, M., et al. (2016). Direct observation of aqueous secondary organic aerosol from biomass-burning emissions. *Proceedings of the National Academy of Sciences, 113*, 10013-10018.

Gilardoni, S., Vignati, E., Cavalli, F., Putaud, J. P., Larsen, B. R., Karl, M., et al. (2011). Better constraints on sources of carbonaceous aerosols using a combined ^{14}C-macro tracer analysis in a European rural background site. *Atmospheric Chemistry and Physics, 11*, 5685-5700.

Glasius, M., Hansen, A. M., Claeys, M., Henzing, J. S., Jedynska, A. D., Kasper-Giebl, A., et al. (2018). Composition and sources of carbonaceous aerosols in Northern Europe during winter. *Atmospheric Environment, 173*, 127-141.

Goldstein, A. H., & Galbally, I. E. (2007). Known and Unexplored Organic Constituents in the Earth's Atmosphere. *Environmental Science & Technology, 41*, 1514-1521.

Gong, S. L. (2003). A parameterization of sea-salt aerosol source function for sub- and super-micron particles. *Global Biogeochemical Cycles, 17*, n/a--n/a.

Grieshop, A. P., Miracolo, M. A., Donahue, N. M., & Robinson, A. L. (2009). Constraining the Volatility Distribution and Gas-Particle Partitioning of Combustion Aerosols Using Isothermal Dilution and Thermodenuder Measurements. *Environmental Science & Technology, 43*, 4750-4756.

Guariso, G., & Sangiorgio, M. (2018). Integrating Economy, Energy, Air Pollution in Building Renovation Plans. *IFAC-PapersOnLine, 51*, 102-107.

Guenther, A., Karl, T., Harley, P., Wiedinmyer, C., Palmer, P. I., & Geron, C. (2006, 8). Estimates of global terrestrial isoprene emissions using MEGAN (Model of Emissions of Gases and Aerosols from Nature). *Atmospheric Chemistry and Physics, 6*, 3181-3210.

Guerreiro, C. B., Foltescu, V., & Leeuw, F. (2014). Air quality status and trends in Europe. *Atmospheric Environment, 98*, 376-384.

Hallquist, M., Wenger, J. C., Baltensperger, U., Rudich, Y., Simpson, D., Claeys, M., et al. (2009). The formation, properties and impact of secondary organic aerosol: current and emerging issues. *Atmospheric Chemistry and Physics, 9*, 5155-5236.

Harrison, R. M., Stedman, J., & Derwent, D. (2008). New Directions: Why are PM_{10} concentrations in Europe not falling? *Atmospheric Environment, 42*, 603-606.

Hatch, L. E., Yokelson, R. J., Stockwell, C. E., Veres, P. R., Simpson, I. J., Blake, D. R., et al. (2017). Multi-instrument comparison and compilation of non-methane organic gas emissions from biomass burning and implications for smoke-derived secondary organic aerosol precursors. *Atmospheric Chemistry and Physics, 17*, 1471-1489.

Hodzic, A., Jimenez, J. L., Madronich, S., Canagaratna, M. R., DeCarlo, P. F., Kleinman, L., et al. (2010). Modeling organic aerosols in a megacity: potential contribution of semi-volatile and intermediate volatility primary organic compounds to secondary organic aerosol formation. *Atmospheric Chemistry and Physics, 10*, 5491-5514.

Hodzic, A., Kasibhatla, P. S., Jo, D. S., Cappa, C. D., Jimenez, J. L., Madronich, S., et al. (2016). Rethinking the global secondary organic aerosol (SOA) budget: stronger production, faster removal, shorter lifetime. *Atmospheric Chemistry and Physics, 16*, 7917-7941.

Jathar, S. H., Cappa, C. D., Wexler, A. S., Seinfeld, J. H., & Kleeman, M. J. (2016). Simulating secondary organic aerosol in a regional air quality model using the statistical oxidation model - Part 1: Assessing the influence of constrained multi-generational ageing. *Atmospheric Chemistry and Physics, 16*, 2309-2322.

Jathar, S. H., Gordon, T. D., Hennigan, C. J., Pye, H. O., Pouliot, G., Adams, P. J., et al. (2014). Unspeciated organic emissions from combustion sources and their influence on the secondary organic aerosol budget in the United States. *Proceedings of the National Academy of Sciences, 111*, 10473-10478.

Jathar, S. H., Woody, M., Pye, H. O., Baker, K. R., & Robinson, A. L. (2017). Chemical transport model simulations of organic aerosol in southern California: model evaluation and gasoline and diesel source contributions. *Atmospheric Chemistry and Physics, 17*, 4305-4318.

Jimenez, J. L., Canagaratna, M. R., Donahue, N. M., Prevot, A. S., Zhang, Q., Kroll, J. H., et al. (2009). Evolution of Organic Aerosols in the Atmosphere. *Science, 326*, 1525-1529.

Karnezi, E., Murphy, B. N., Poulain, L., Herrmann, H., Wiedensohler, A., Rubach, F., et al. (2018). Simulation of Atmospheric Organic Aerosol using its Volatility-Oxygen Content Distribution during the PEGASOS 2012 campaign. *Atmospheric Chemistry and Physics Discussions, 2018*, 1-31.

Kim, Y., Sartelet, K., Seigneur, C., Charron, A., Besombes, J.-L., Jaffrezo, J.-L., Marchand, N., Polo, L. (2016). Effect of measurement protocol on organic aerosol measurements of exhaust emissions from gasoline and diesel vehicles. *Atmospheric Environment, 140*, 176-187.

Koo, B., Knipping, E., & Yarwood, G. (2014). 1.5-Dimensional volatility basis set approach for modeling organic aerosol in CAMx and CMAQ. *Atmospheric Environment, 95*, 158-164.

Lane, T. E., Donahue, N. M., & Pandis, S. N. (2008). Simulating secondary organic aerosol formation using the volatility basis-set approach in a chemical transport model. *Atmospheric Environment, 42*, 7439-7451.

May, A. A., Levin, E. J., Hennigan, C. J., Riipinen, I., Lee, T., Collett, J. L., et al. (2013c). Gas-particle partitioning of primary organic aerosol emissions: 3. Biomass burning. *Journal of Geophysical Research: Atmospheres, 118*, 11,327--11,338.

May, A. A., Presto, A. A., Hennigan, C. J., Nguyen, N. T., Gordon, T. D., & Robinson, A. L. (2013a). Gas-particle partitioning of primary organic aerosol emissions: (1) Gasoline vehicle exhaust. *Atmospheric Environment, 77*, 128-139.

May, A. A., Presto, A. A., Hennigan, C. J., Nguyen, N. T., Gordon, T. D., & Robinson, A. L. (2013b). Gas-Particle Partitioning of Primary Organic Aerosol Emissions: (2) Diesel Vehicles. *Environmental Science & Technology, 47*, 8288-8296.

Meroni, A., Pirovano, G., Gilardoni, S., Lonati, G., Colombi, C., Gianelle, V., et al. (2017). Investigating the role of chemical and physical processes on organic aerosol modelling with CAMx in the Po Valley during a winter episode. *Atmospheric Environment, 171*, 126-142.

Middlebrook, A. M., Bahreini, R., Jimenez, J. L., & Canagaratna, M. R. (2012). Evaluation of Composition-Dependent Collection Efficiencies for the Aerodyne Aerosol Mass Spectrometer using Field Data. *Aerosol Science and Technology, 46*, 258-271.

Murphy, B. N., & Pandis, S. N. (2009). Simulating the Formation of Semivolatile Primary and Secondary Organic Aerosol in a Regional Chemical Transport Model. *Environmental Science & Technology, 43*, 4722-4728.

Ng, N. L., Herndon, S. C., Trimborn, A., Canagaratna, M. R., Croteau, P. L., Onasch, T. B., et al. (2011). An Aerosol Chemical Speciation Monitor (ACSM) for Routine Monitoring of the Composition and Mass Concentrations of Ambient Aerosol. *Aerosol Science and Technology, 45*, 780-794.

Odum, J. R., Hoffmann, T., Bowman, F., Collins, D., Flagan, R. C., & Seinfeld, J. H. (1996). Gas/Particle Partitioning and Secondary Organic Aerosol Yields. *Environmental Science & Technology, 30*, 2580-2585.

Ots, R., Young, D. E., Vieno, M., Xu, L., Dunmore, R. E., Allan, J. D., et al. (2016). Simulating secondary organic aerosol from missing diesel-related intermediate-volatility organic compound emissions during the Clean Air for London (ClearfLo) campaign. *Atmospheric Chemistry and Physics, 16*, 6453-6473.

Pepe, N., Pirovano, G., Lonati, G., Balzarini, A., Toppetti, A., Riva, G. M., et al. (2016). Development and application of a high resolution hybrid modelling system for the evaluation of urban air quality. *Atmospheric Environment, 141*, 297-311.

Pernigotti, D., Georgieva, E., Thunis, P., & Bessagnet, B. (2012). Impact of meteorology on air quality modeling over the Po valley in northern Italy. *Atmospheric Environment, 51*, 485-490.

Perrino, C., Catrambone, M., Dalla Torre, S., Rantica, E., Sargolini, T., & Canepari, S. (2014). Seasonal variation in the chemical composition of particulate matter: a case study in the Po Valley. Part I: macro-components and mass closure. *Environ. Sci. Pollut. Res., 21*, 3999-4009.

Pietrogrande, M. C., Bacco, D., Ferrari, S., Kaipainen, J., Ricciardelli, I., Riekkola, M.-L., et al. (2015). Characterization of atmospheric aerosols in the Po valley during the supersito campaigns — Part 3: Contribution of wood combustion to wintertime atmospheric aerosols in Emilia Romagna region (Northern Italy). *Atmospheric Environment, 122*, 291-305.

Robinson, A. L., Donahue, N. M., Shrivastava, M. K., Weitkamp, E. A., Sage, A. M., Grieshop, A. P., et al. (2007). Rethinking Organic Aerosols: Semivolatile Emissions and Photochemical Aging. *Science, 315*, 1259-1262.

Sartelet, K., Zhu, S., Moukhtar, S., André, M., André, J.M., Gros, V., Favez, O., Brasseur, A., Redaelli, M. (2018). Emission of intermediate, semi and low volatile organic compounds from traffic and their impact on secondary organic aerosol concentrations over Greater Paris. *Atmospheric Environment, 180*, 126-137.

Schauer, J. J., Kleeman, M. J., Cass, G. R., & Simoneit, B. R. (1999). Measurement of Emissions from Air Pollution Sources. 2. C1 through C30 Organic Compounds from Medium Duty Diesel Trucks. *Environmental Science & Technology, 33*, 1578-1587.

Shrivastava, M., Fast, J., Easter, R., Gustafson Jr., W. I., Zaveri, R. A., Jimenez, J. L., et al. (2011). Modeling organic aerosols in a megacity: comparison of simple and complex representations of the volatility basis set approach. *Atmospheric Chemistry and Physics, 11*, 6639-6662.

Skamarock, W. C., Klemp, J. B., Dudhia, J., Gill, D. O., Barker, D. M., Wang, W., et al. (2008). A description of the Advanced Research WRF version 3. NCAR Technical note -475+STR.

Strader, R., Lurmann, F., & Pandis, S. N. (1999). Evaluation of secondary organic aerosol formation in winter. *Atmospheric Environment, 33*, 4849-4863.

Tsimpidi, A. P., Karydis, V. A., Zavala, M., Lei, W., Bei, N., Molina, L., et al. (2011). Sources and production of organic aerosol in Mexico City: insights from the combination of a chemical transport model (PMCAMx-2008) and measurements during MILAGRO. *Atmospheric Chemistry and Physics, 11*, 5153-5168.

Tsimpidi, A. P., Karydis, V. A., Zavala, M., Lei, W., Molina, L., Ulbrich, I. M., et al. (2010). Evaluation of the volatility basis-set approach for the simulation of organic aerosol formation in the Mexico City metropolitan area. *Atmospheric Chemistry and Physics, 10*, 525-546.

WHO. (2006). *WHO air quality guidelines for particulate matter, ozone, nitrogen dioxide and sulfur dioxide - global update 2005 - summary of risk assessment* . World Health Organization, Copenhagen, Denmark.

Woody, M. C., Baker, K. R., Hayes, P. L., Jimenez, J. L., Koo, B., & Pye, H. O. (2016). Understanding sources of organic aerosol during CalNex-2010 using the CMAQ-VBS. *Atmospheric Chemistry and Physics, 16*, 4081-4100.

Woody, M. C., West, J. J., Jathar, S. H., Robinson, A. L., & Arunachalam, S. (2015). Estimates of non-traditional secondary organic aerosols from aircraft SVOC and IVOC emissions using CMAQ. *Atmospheric Chemistry and Physics, 15*, 6929-6942.

Yarwood, G., Jung, J., Whitten, G. Z., Heo, G., Mellberg, J., & Estes, E. (2010). *Updates to the Carbon Bond Mechanism for Version 6 (CB6).* Presented at the 9th Annual CMAS Conference, Chapel Hill, NC, October 11-13, 2010 .

Zhang, Q. J., Beekmann, M., Drewnick, F., Freutel, F., Schneider, J., Crippa, M., et al. (2013). Formation of organic aerosol in the Paris region during the MEGAPOLI summer campaign: evaluation of the volatility-basis-set approach within the CHIMERE model. *Atmospheric Chemistry and Physics, 13*, 5767-5790.

Zhang, Q., Jimenez, J. L., Canagaratna, M. R., Allan, J. D., Coe, H., Ulbrich, I., et al. (2007). Ubiquity and dominance of oxygenated species in organic aerosols in anthropogenically-influenced Northern Hemisphere midlatitudes. *Geophysical Research Letters, 34*, n/a--n/a.

Zhang, X., Cappa, C. D., Jathar, S. H., McVay, R. C., Ensberg, J. J., Kleeman, M. J., et al. (2014). Influence of vapor wall loss in laboratory chambers on yields of secondary organic aerosol. *Proceedings of the National Academy of Sciences, 111*, 5802-5807.

Zhao, Y., Nguyen, N. T., Presto, A. A., Hennigan, C. J., May, A. A., & Robinson, A. L. (2015). Intermediate Volatility Organic Compound Emissions from On-Road Diesel Vehicles: Chemical Composition, Emission Factors, and Estimated Secondary Organic Aerosol Production. *Environmental Science & Technology, 49*, 11516-11526.

Zhao, Y., Nguyen, N. T., Presto, A. A., Hennigan, C. J., May, A. A., & Robinson, A. L. (2016). Intermediate Volatility Organic Compound Emissions from On-Road Gasoline Vehicles and Small Off-Road Gasoline Engines. *Environmental Science & Technology, 50*, 4554-4563.